Journal of Public Economics 223 (2023) 104904

Contents lists available at ScienceDirect

Journal of Public Economics

journal homepage: www.elsevier.com/locate/jpube

Disguised pollution: Industrial activities in the dark ☆

Sumit Agarwal [a,*], Yajie Han [b], Yu Qin [b], Hongjia Zhu [c]

[a] School of Business, and School of Arts and Social Science, National University of Singapore, Singapore
[b] Department of Real Estate, National University of Singapore, Singapore
[c] Institute for Economic and Social Research, Jinan University, Guangzhou, China

ARTICLE INFO

Article history:
Received 20 August 2022
Revised 11 April 2023
Accepted 27 April 2023
Available online 17 May 2023

JEL Codes:
Q53
L51
I18
D22

Keywords:
Air pollution
Disguised behavior
Industrial firm
Inspections
China

ABSTRACT

In this study we investigate disguised pollution by industrial firms in China. We find that sulfur dioxide (SO_2) readings increase by 10.8% in air pollution monitoring stations four hours after sunset in high factory density areas, controlling for station-year, date, and city-hour fixed effects. Physical inspections by the Ministry of Environmental Protection may only temporarily reduce disguised pollution, suggesting that reliance on physical inspections to enforce regulations is ineffective if firms can shift production activities to non-daylight hours. We show that direct monitoring, as is done with some large polluters in China, can prevent this and should be cost-effective to extend to all industrial polluters.

1. Introduction

Firms will go to great lengths to circumvent regulatory oversight as regulatory compliance is costly and subject to pressure from multiple stakeholders (Henriques and Sadorsky, 1996). In this paper, we show that some Chinese firms, under cover of darkness, emit increased amounts of sulfur dioxide (SO_2).[1] There are two reasons why firms might increase non-compliant production, and thereby pollution, outside of daylight hours. First, emissions are visible in the daytime, especially sulfide compounds with a yellowish color, so nearby residents may complain to their local environmental bureaus if they see the smoke, and inspectors from the local environmental bureaus can impose fines on the firms if they can confirm that illegal emissions are occurring. However, emissions at night are much less visible and inspectors are less likely to be on duty at night, implying a lower probability of complaints, detection, governmental inspection, and fines. Second, desulfurization is very costly. Variable costs including electricity, water, desulfurizer, and steam are a few times higher than the annual depreciation costs of the equipment (Wu et al., 2015). Therefore, firms have an incentive to

☆ We thank the editor and three anonymous referees for their valuable comments and suggestions. We are also grateful for valuable comments from Douglas Almond, Gene Amromin, Adonis Antoniades, Souphala Chomsisengphet, Tatyana Deryugina, Roger von Hafen, Guojun He, Ruixue Jia, Ashley Langer, Shanjun Li, Abhiroop Mukharjee, Wenlan Qian, David Reeb, Alberto Salvo, Juan Zhang, Junjie Zhang, Peng Zhang, Huanhuan Zheng, Joshua Graff Zivin, Eric Zou, and seminar participants at Chinese University of Hong Kong, Hong Kong Baptist University, Peking University, Renmin University, Hong Kong University of Science and Technology, Tsinghua University, National University of Singapore and Sun Yat-Sen University. The authors acknowledge research assistance from Hui Hu, Jieye Chen, Ling Wang, Wenwen Qian, Siyu Liu, and Zhichao Tang. Sumit Agarwal acknowledges funding support from Low Tuck Kuang Research Grant; Sumit Agarwal and Yu Qin acknowledge funding support from New Energy Research R&D (R-315–000-132–720); Hongjia Zhu acknowledges funding support from National Natural Science Foundation of China (72003078), Fundamental Research Funds for the Central Universities (17 JNQN015). All authors contribute equally. All errors remain ours.

* Corresponding author.
E-mail addresses: ushakri@yahoo.com (S. Agarwal), yajie.h@u.nus.edu (Y. Han), bizqyu@nus.edu.sg (Y. Qin), zhuhjecon@hotmail.com (H. Zhu).

[1] Anecdotal evidence of firms' disguised pollution at night has been reported in the news (for example, https://www.chinanews.com/gn/2015/03–10/7117032.shtml (accessed on 20 Dec 2022); https://www.chinacourt.org/article/detail/2013/07/id/1039669.shtml (accessed on 20 Dec 2022), and even in the Report on the Work of the Government by Premier Li Keqiang (https://www.gov.cn/guowuyuan/2015–03/16/content_2835101.htm, accessed on 20 Dec 2022).

https://doi.org/10.1016/j.jpubeco.2023.104904
0047-2727/

shut down the desulfurization equipment at night when the chance of this being detected is much lower.

Our investigation was prompted by two stylized facts. First, if we take a snapshot of SO_2 pollution across all the 1,583 air pollution monitoring stations in China after controlling for time and weather (Fig. A1), we find contrasting patterns in autumn and winter (Oct-Apr), and spring and summer (Apr-Oct). During the winter, SO_2 is higher in the north, while during the summer, SO_2 is higher in the south. Second, if we plot the average readings of SO_2 before and after sunset time at each station, we observe a significant rise in SO_2 after sunset. However, this could be due to various factors: operational practices, weather conditions, winter heating, and firm manipulation of pollution emissions. SO_2 emission is also largely affected by the industrial structure of an area, which in turn is driven by the economic make up of a city. In addition, the increase in SO_2 may be driven by atmospheric conditions instead of firms' behavioral changes: sunlight can interact with pollutants and facilitate secondary chemical effects. Lastly, lower temperatures after sunset may affect the dissipation of pollutants.

To make a causal argument of nightfall and increased pollution, we use the variation in sunset times across China and the hourly recording of pollution levels across all 1,583 monitoring stations from 2015 to 2017. These national monitoring stations are installed in various locations in China and our data is the aggregate of these stations. Not all stations are located near pollutant emitting firms; approximately a quarter of them are located near non-industrial areas. This variation allows us to compare the pollution readings in monitoring stations with high factory density in the surrounding area and stations with low factory density in the surrounding area, before and after sunset, giving us a clean difference-in-differences analysis and supporting the causal argument for the intentional increase of pollution emissions under the disguise of the night.

The thought experiment we have in mind requires that there are two monitoring stations in the same city—one in the industrial area and the other in the non-industrial area. After sunset, the probability of inspection is lower, thus firms may shut down the desulfurization equipment that lowers the SO_2 emissions to reduce costs, and/or increase production activities that cause higher levels of SO_2 emissions and thus increase profits. However, there is no change in the emission levels in the non-industrial areas which experience sunset at the same time. City-hour and station-year fixed effects allow us to cleanly get to our experiment, which rules out both time-variant (such as electricity prices) and time-invariant city-level unobservables, as well as year-variant station-level unobservables. In addition, we flexibly control for the atmospheric conditions that may affect the dissipation of pollutants before and after sunset, including precipitation, wind speed and direction, temperature, dew point, daily range of temperature, boundary layer height, and surface pressure.

We found that there is a 10.8% increase in SO_2 emission levels in the four hours after sunset in comparison to the six hours before sunset as measured by monitoring stations near the industrial areas as opposed to stations near the residential areas, which translates into an hourly difference of 6.3% before and after sunset. Most importantly, our results are robust to different confounders, including changes in atmospheric conditions post-sunset (such as the change of the boundary layer height), changes in electricity generation and electricity prices within a day, production shifts within a day, winter heating, and traffic flows. Besides, we find that the gap between the two groups gradually narrows around sunrise. Considering the possibility that monitoring stations are likely to be placed in relatively cleaner areas (Grainger et al., 2018), our estimates on disguised pollution may be lower than what actually occurs.

Moreover, we find that the level of disguised pollution at night varies with political factors such as political turnover and central inspection. Disguised pollution is 54.0–61.9% higher in a half year after the turnover of the municipal party secretary, compared to periods before the turnover, and such effect is less pronounced if the new party secretary has environmental governance experience. We also show that inspections by the Ministry of Environmental Protection (MEP) after 2014 may only decrease the disguised pollution temporarily during MEP officials' stay. Such activity reverts to previous levels after the MEP officials leave the sites.[2] Finally, we show that disguised pollution is inversely correlated with pressures due to a local economic downturn. A one percentage decline in GDP growth rate in the previous year increases the magnitude of disguised pollution in the current year by 11.1–12.7%. Such findings also support our argument that the effect is not due to atmospheric conditions, otherwise it should not vary with political turnover, central inspection, or local economic growth. Furthermore, we do not find evidence that the firms that are deemed to be high polluters and as a result have individual monitoring devices installed, increase their emissions at night. However, we do find that firms in key regions that are more strictly monitored are less likely to underreport their emissions readings after sunset than firms in non-key regions, though the magnitude of such difference is small.

This paper contributes to the current literature in four ways. First, our paper adds to the discussion regarding the gaps between regulation enforcement and actual pollution abatement. Specifically, we provide novel evidence for firms' short-term strategic actions in the context of point-source non-automated monitoring and imperfect inspection by the regulators. There is also emerging literature on the agencies' evasive responses to environmental regulations. For example, Vollaard (2017) demonstrates evidence of the illegal discharge of oil from shipping vessels under the cover of darkness in the Dutch part of the North Sea. Additionally, Zou (2021) documents increases in polluting activities during unmonitored times due to a "once-every-six-days" air quality monitoring schedule under the federal Clean Air Act. Alexander and Schwandt (2022) utilize emission-cheating diesel cars to study the impact of car pollution on infant health. Our paper contributes to this stream of literature by showing that without point-source level surveillance technologies, these evasive behaviors could still occur even if there is a nationwide network of automated monitoring systems. Moreover, the intensity of evasive behaviors is associated with a variety of socioeconomic factors such as local economic growth pressure and political turnover.

Second, our paper contributes to empirical evidence in evaluating the effects of environmental inspections. Using the event study approach, a large body of literature sheds light on the question of whether inspections conducted by environmental regulators can reduce plant emissions in the long run. For instance, Eckert (2004) finds that in petroleum storage sites in Canada, inspections can deter future violations but the effect is small. However, Keohane et al. (2009) explore the case of the US electric power industry and find that the threat of enforcement has a notable effect on the firms' emissions.[3] Furthermore, Hanna and Oliva (2010) show that an inspection under the Clean Air Act can lead to a decrease in plant emission by around 15%, and that this effect is stronger for those industries having low abatement costs. Note that most of the previous studies focus on firms' subsequent response

[2] Using the National Specially Monitored Firms (NSMF) Program implementation as a quasi-experiment, Zhang et al. (2018a) also find that direct central supervision by the MEP substantially reduced industrial water pollution by more than 26% in the short term.

[3] Similar findings are also demonstrated in Shimshack and Ward (2008), who show that increased enforcement even causes over-compliance in the non-inspected firms. Shimshack (2014) provides a detailed review of some recent studies focusing on the effect of inspection and governmental enforcement on pollution.

after an actual inspection in the long run, while we provide evidence from a short run perspective that firms may also react to changes in inspection probability within a day.

Third, this paper contributes to the literature on environmental regulation policies in developing countries. Most of the existing environmental regulation studies focus on North American and European countries, while discussions in the context of the developing world are relatively rare. However, because both inspection and compliance are costly (He et al., 2020; Shimshack, 2014), and developing countries typically face higher pollution levels, tighter budget constraints, and weaker law enforcement institutions (e.g., due to corruption), it is important to understand how firms respond to different monitoring tools in the developing world. For instance, Duflo et al. (2018) examine the effects of different inspection policies on plant emissions in India and find that targeted inspections have a much stronger effect than random inspections. Our paper, however, shows that in China, a continuous monitoring system is more effective than inspections. This is also related to the discussions by Karplus et al. (2018), which find a reduction of SO_2 emissions following the implementation of tougher national air emissions standards in coal power plants being monitored by Continuous Emissions Monitoring Systems (CEMS). Our results further support their argument that monitoring practices with high-quality data are very important for pollution abatement.

Finally, our paper is related to the work on using administrative data and other new data sources to identify disguised behaviors. Drawing upon data on pollution monitoring and pollution alerts, Mu et al. (2021) find that local governments in the US strategically skip air pollution monitoring in order to meet federal air quality standards. Agarwal et al. (2020) identify disguised corruption from credit card transaction data. Finer (2018) employs taxi data to identify possible information leakage from Federal Reserve meetings. Deng et al. (2015) infer the unreported income of government officials from housing purchase data. Our paper is the first to uncover firms' pollution behavior under the cover of night, using high-frequency station-level and firm-level monitoring data. From the perspective of practical surveillance, our results also suggest that a closer look into high-frequency station level monitoring data could identify the areas that are worth stricter enforcement efforts.

The paper proceeds as follows. Section 2 introduces the background of interaction between industrial firms and regulators related to evasive emission issues in China; Section 3 discusses the data sources used in the analysis; Section 4 describes the identification strategies; Sections 5 and 6 present the main findings and discussion; Section 7 concludes.

2. Background

2.1. Firm incentives to discharge SO_2 under the cover of darkness

Sulfur widely exists in industrial fuels, and the combustion of such fuels inevitably results in the production of waste off-gases containing a range of sulfur compounds. Among these, SO_2 is one of the most concerning pollutants as it has been shown to cause serious negative health issues. It is estimated that the industrial sector accounts for the biggest share of sulfur dioxide emissions in China. On the one hand, the concentration of SO_2 in the off-gases largely depends on the sulfur content in different fuels, which generally ranges from 1.5% to 4% (Sun et al., 2016). To deal with this problem, in recent years the Chinese government has adopted various policies to force or incentivize industrial firms, particularly coal-fired power plants, to upgrade their boiler technologies or to enhance fuel standards. On the other hand, even the most up-to-date commercially-used technologies could still produce exhaust gases containing pollutants that easily exceed the regulatory levels. Therefore, the environmental regulators also require the polluting firms to install end-of-pipe pollutant scrubbers, which are expected to significantly reduce pollutant concentrations in the discharges.

However, the installment of end-of-pipe pollutant scrubbers is not cheap. More importantly, the operating costs of such equipment are also not negligible. Karatepe (2000) provides a detailed comparison of the economic costs of different flue gas desulfurization processes, while Sun et al. (2016) introduce some new advanced technologies that could be commercially applied. In general, there are two major categories of desulfurization technologies based on the mechanisms of sulfur dioxide removal: wet scrubbing and dry scrubbing. Under these two process types, different sorbent materials are used and most of them produce different final wastes that require transport and storage. For instance, limestone and lime are the two most popular sorbents to remove sulfur dioxide in industries, however, they are not regenerative and produce a substantial amount of gypsum/lime sludge which is difficult for firms to dispose of, further adding to the running costs of the scrubbers.

Since the end-of-pipe desulfurization scrubber is usually a piece of stand-alone equipment that can be switched on and off by the firms during the production process, the high operating costs of such scrubbers incentivize firms to shut down the scrubbers in some circumstances. In this case, the waste off-gases without any pollutant removal process would appear very different to the cleaner discharges. For example, besides the colorless sulfur dioxide, the combustion of coal also results in a variety of other sulfur compounds that have a yellowish color, so that discharging the off-gases from the chimneys directly could be easily spotted by regulators. To circumvent potential inspections during the daytime, it has been reported that many firms choose to shut down the scrubbers at night.[4]

2.2. Regulators' reaction to the evasive emissions

To curb the massive SO_2 emissions seen in the 1990 s, China's central government implemented a number of policies and introduced new instruments starting in 2001 (the beginning of its 10th Five-year Plan), including market-based instruments, command-and-control, and administrative instruments. These policy instruments effectively reduced SO_2 emissions by 28% from 2001 to 2005, and a further 14% from 2006 to 2010 (Schreifels et al., 2012).

Amidst the recent regulatory policies, two control measures are deemed to directly influence firms' pollution abatement behavior. The first is the implementation of CEMS at the above-scale polluters to collect real-time emission data. The CEMS, which is installed in the chimney, is designed to be independent of the operation of scrubbers and can transmit real-time readings of three major pollutants in end-of-pipe off-gases, including SO_2, TSP, and NO_x, to the data center of the MEP. But CEMS has some limitations that may dampen its effectiveness: first, the installment and maintenance costs are high, so it is currently only adopted by large firms. Therefore, as the small- and medium-sized firms usually have lower production and pollutant removal technologies, they have strong incentives to disguise their polluting behavior. This would imply that the low distribution of CEMS could have overlooked an important group of targets; additionally, even though ideally CEMS can have automated monitoring functions, firms can still interfere with the operation of CEMS by various means. The effectiveness of CEMS is closely related to the local regulatory pressures. For example, Karplus et al. (2018) document a weak

[4] There is anecdotal evidence that power plants have installed expensive desulfurization equipment, but have not put it into use alongside their generating units (see https://news.sina.com.cn/c/2006–05-23/03389936463.shtml, accessed on 20 Dec 2022).

association between the SO_2 measurements of coal power plants reported from CEMS and the observation from satellite data in key regions facing the toughest new emission standards, indicating that the coal power plants may game the system with the MEP on reported data quality when facing high regulatory pressures.[5]

The other regulatory measure that is taken to enforce firms' abatement is inspection by local bureaus and the central government. With the constraints of a limited workforce, it is impractical for local environmental protection bureaus to send out surveillance teams to cover all pollution hotspots within their jurisdictions. Instead, local regulators often rely on reports of suspicious environmental issues from local residents via a variety of channels such as social media (e.g., Weibo, WeChat) or official online message boards (e.g., "Message Board for Local Leaders"). After collecting information from these sources, a team of officers will visit the venue to collect evidence with pollutant detecting instruments or to conduct an indoor production environment check. However, there are serious weaknesses in this workflow: it relies heavily on neighborhood alerts, and these are likely to be much less common in the nighttime. In addition, there is a time lag between observing pollutant discharges and evidence collection, making it difficult to catch offenders in the act.

After a wide search for anecdotal news and official documents about local environmental protection authorities' enforcement practices, we have established two facts. First, local authorities recognize the existence of firms' illegal discharge behavior. Second, as a complement to the other measures such as CEMS monitoring or regular surveillance on industrial sites, they conduct irregular inspections at night.[6] Moreover, to strengthen the enforcement of environmental protection law, the MEP conducted inspections across all provinces in China from December 2015 to August 2017 in a few waves, thus setting in motion the first comprehensive centralized environmental inspection program in China. The inspection team stayed in each province for one month to investigate pollution issues in that province. More than 5,000 inspectors were dispatched to local sites during this period.[7] It is reported that the MEP inspection teams also conducted nightly inspections, especially for notorious polluting areas such as Hebei Province.[8] However, given the large number of industrial firms in China, even thousands of inspectors are not likely to be able to regularly cover all the polluting sites, especially if the firms game the inspectors by disguising their polluting behavior, which is the study scope of this paper.

3. Data sources

We draw data from three sources. First, we use the hourly pollution data from the 1,583 national monitoring stations in China from January 2015 to December 2017.[9] The data reports hourly readings of six pollutants, including SO_2, $PM_{2.5}$, PM_{10}, NO_2, CO, and O_3. In addition, an hourly air quality index (AQI) measure is available, which is a composite index of multiple pollutants. Fig. A2 shows the average hourly readings of SO_2 across all stations. According to the WHO standard, exposure to 20 $\mu g/m^3$ SO_2 or higher on a 24-hour average may lead to negative health consequences. However, large areas in China, especially Northern China, have an average hourly SO_2 that is above 20 $\mu g/m^3$.

We focus on SO_2 rather than other pollutants for the following reasons. The effect and amount of CO is confounded by vehicle emissions, and industrial sites are likely to be located in areas with a higher density of road networks and vehicles.[10] Thus the increase in CO may not be solely attributable to the disguised pollution of industrial firms. We do not discuss NO_2 and O_3 in this paper because the effect of sunset on these two pollutants is ambiguous: NO_2 and NO can equilibrate within a few minutes (and react with O_3) in the presence of sunlight (Rohde and Muller, 2015). Given that our pollutant data source measures NO_2 instead of NO_x, it is not clear whether the change in NO_2 is due to industrial emission, or the change in chemical effects with other pollutants, such as O_3, after sunset. Along the same lines, we do not discuss $PM_{2.5}$ and PM_{10} because they are not only emitted directly from construction sites, dusty roads, and agricultural activities but are also formed in the atmosphere through complex chemical reactions that interact with sunlight (Zhang and Cao, 2015).

To understand the surroundings of each monitoring station, we search all the points of interest (POIs) within a 3 km radius of each station using AutoNavi Map.[11] We then count the number of factories within 3 km of each monitoring station, and the number of factories involved in SO_2-intensive industries, including production and supply of electric power and heat power, metal-related industries, raw chemical materials, chemical products, and petroleum processing industries (Chen et al., 2018).[12] We also merge the station-level pollution data with the hourly weather conditions near the station, including precipitation, wind speed, wind direction, dew point, temperature, surface pressure, and boundary layer height.[13] Following

[5] Duflo et al. (2013) also find evidence of manipulation of reported data in the status quo system in India, however, they show that the third-party auditors can substantially improve the reliability of the audit reports.

[6] See https://www.xinhuanet.com/politics/2016–12/05/c_1120053568.htm (acessed on 25 Mar 2023) for an anecdotal example of the irregular inspection at night.

[7] See https://www.xinhuanet.com//2017–05/09/c_1120942953.htm (accessed on 20 Apr 2018).

[8] See a news report on nightly inspection from https://www.chinanews.com.cn/sh/2016/12–05/8083330.shtml (accessed on 20 Dec 2022).

[9] Our data is downloaded from https://beijingair.sinaapp.com/, the data source of which is the National Urban Air Quality Live Update Platform (https://106.37.208.233:20035/). In addition to the pollutant measures, the National Urban Air Quality Live Update Platform provides the geographic coordinates of each monitoring station. We have compared our downloaded data with the historical data published by MEP. They are consistent with each other. People may worry that firms may bribe the MEP to forge the data in monitoring stations. This is captured by the station-day fixed effect and will not bias our estimate as long as the data manipulation effort is not correlated with sunset time, which is unlikely.

[10] Vehicle emissions may also contain some sulfur dioxide especially if fuel quality is low. However, vehicle emissions will not bias our estimate as long as vehicle emissions are not correlated with sunset time within a city. As far as we know, major cities in China usually impose restrictions on the entry of heavy vehicles (such as diesel trucks) in urban areas based on clock time (for instance, after 10pm and before 7am daily) instead of sunset time.

[11] We identify the Points of Interest (POIs) near each monitoring station using AutoNavi Map (https://www.autonavi.com/#/) API. It searches a 3 km radius around each air quality monitor station and returns a list of the name and associated coordinates that are labelled as "industrial firms". The source code is available upon request. The coordinates of the POIs are finally transferred to the WGS84 coordinate system for geographical matching and computation.

[12] We identify SO_2 intensive industries (available in appendix Table A.1 of Chen, Li and Lu (2018)) by searching the names of the factories with the following keywords: "*huagong*" (raw chemical materials and chemical products), "*jinshu*" (pressing of ferrous metals), "*dianli*" (production and supply of electric power & heat power), "*yelian*" (pressing of ferrous metals), "*shiyou*" (processing of petroleum), "*shihua*" (processing of petroleum), "he"(pressing of nuclear fuel), and "*mei*" (non-metallic mineral products).

[13] Our first weather dataset is from National Oceanic and Atmospheric Administration, which provides global hourly records at the monitor station level in their archive (https://www.ncei.noaa.gov/data/global-hourly/). There are 386 stations in total with valid hourly readings within China from 2015 to 2017. The dataset contains essential descriptions of the monitor stations such as station id, station name, reported hour, and longitude and latitude, which enable us to link the air quality data by time and distance with the nearest air quality monitor station. Additionally, it provides rich information on the hourly weather conditions including air temperature, wind speed, dew point, and precipitation, etc. It is noted that for the stations which report the readings every three hours, in order to merge with our hourly air quality data, we fill the missing values by applying a linear interpolation. Our second weather dataset is ERA5, from which we retrieve hourly boundary layer height and surface pressure during 2015–2017. It provides hourly estimates of a large number of atmospheric, land and oceanic climate variables. The data has a resolution of 0.25 degrees×0.25 degrees.

the method suggested by Corripio (2003), we obtain the daily sunset time based on latitude, longitude and date for each monitoring station. We define the hour during which sunset happens as the sunset hour. For example, if the sunset time is 4:15 pm, then the sunset hour is from 4 pm to 5 pm. Then, 5–6 pm is defined as one hour after sunset, 6–7 pm is defined as two hours after sunset, etc. Fig. A3 shows the sunset hours by longitudes in winter and summer.

Table 1 presents the summary statistics of the first and the last quintile in terms of the average number of SO_2 factories. For monitoring stations in the bottom 20%, on average, there is no SO_2-producing factory within a 3 km radius. However, for monitoring stations at the top 20%, on average there are 3.21 SO_2-producing factories within a 3 km radius. Panel B provides the average and standard deviation of pollutants and atmospheric conditions six hours before and four hours after sunset for each group. From a simple comparison of the raw data before and after sunset without any regression adjustment, we observe an approximately 5% decrease in SO_2 after sunset for both groups. In general, the atmospheric conditions change similarly after sunset for stations at the bottom 20% and top 20%, with lower temperatures, slower wind speeds, higher dew temperatures, slightly more precipitation, and lower boundary layer height after sunset.

Our second data source is from the high-frequency monitoring data of 135 factories in Shijiazhuang, Qinhuangdao, and Tangshan in Hebei Province, and 177 factories in Zhejiang Province in 2015. The Continuous Emissions Monitoring Systems (CEMS) implemented by the Ministry of Environmental Protection (MEP) involve the installation of monitors in factories among key industrial sectors that contribute most of the industrial pollution. The purpose of establishing the CEMS is to facilitate better information disclosure and promote public participation in pollution monitoring. Firms that fail to comply with the CEMS monitoring practice incur severe penalties such as suspension of new project approval, suspension of environmental subsidies, and disqualification as government vendors.[14] The 312 factories in our sample are a comprehensive list in the cities covered by CEMS that monitors major air pollutants, including SO_2, Total Suspended Particles (TSP), and Nitrogen Oxides (NO_x).

Table 1 Panel C presents the summary statistics for the firm-level analysis, reporting the hourly SO_2 and compliance rate before and after sunset for firms covered by CEMS. Information on the hourly emission of SO_2, and on whether the emissions in a certain hour are above the regulated threshold, is directly accessible from the data. We use this to define a new outcome variable, firm compliance, a dummy variable equal to one if the hourly observations measured by CEMS are available and below the emission standard, otherwise zero. We find the compliance rate of firms in non-key regions that are less strictly monitored drops slightly after sunset, whereas the compliance rate of firms in key regions rises slightly. Additionally, a slight increase in SO_2 emissions is observed for firms in non-key regions after sunset, whereas a slight decrease is observed for firms in key regions.

Our third data source is from the Chinese political leader database, which contains information on more than 6,000 Chinese prefectural leaders (municipal party secretaries and mayors) who have served in Chinese prefectural-level and county-level cities since the 1990s. The dataset contains extensive information about these leaders, including their age, education, and work experience before the current appointment. The data also tracks the month and year in which they took and/or left office. We do not distinguish the nature of the officials' turnover, which means we always code a city as having undergone a leadership turnover regardless of whether the former leader was retired, promoted, or laterally moved. We then aggregate the leader-position-year-month-level data into city-level data, which records the year-month of leaders' turnover for each city. The officials' turnover is widely distributed through all months of the year. In our sample from 2015 to 2017, 174 cities experienced at least one turnover of party secretary, and 189 cities experienced at least one change of mayor. On average, the party secretary of each city changed 0.72 times during the sample period of 2015–2017, and the mayor changed 0.68 times.

[14] More details are available in the official document: https://www.mee.gov.cn/gkml/hbb/bgth/ 201305/W020130509639333101097.pdf (accessed on 20 Dec 2022).

4. Identification strategy

We study the effect of sunset on firms' pollution behavior using both station-level analysis and firm-level analysis. For station-level analysis, we adopt a difference-in-differences setting with high dimensional fixed effects. Specifically, we compare the SO_2 readings in stations in the top 20% with stations in the bottom 20% (in terms of both the density of factories overall and the density of factories in SO_2 intensive industries), before and after sunset, conditional on city-by-hour, station-by-year and date fixed effects and weather variables. The regression equation is as follows:

$$P_{i,t} = \beta Sunset_{i,t} \times T_i + \delta Sunset_{i,t} + \lambda \times W_{i,t} + \alpha_{i,r} + \mu_{c,h} + \delta_d + \varepsilon_{i,t} \tag{1}$$

where $P_{i,t}$ denotes the pollution level (in log form) in station i, time t; $Sunset_{i,t}$ takes value 1 if time t in station i is after sunset, otherwise 0; T_i takes value 1 if station i belongs to the treatment group, otherwise 0; $W_{i,t}$ denotes a vector of atmospheric controls for station i, time t, including precipitation, wind speed, wind direction, temperature, dew point, daily range of temperature, boundary layer height, and surface pressure; $\alpha_{i,r}$ stands for station-by-year fixed effects to absorb the station characteristics that change by year such as annual technology updates of monitoring stations and economic growth of the city; $\mu_{c,h}$ represents city-by-hour fixed effects to capture transportation policy shifts and electricity price changes; and δ_d denotes the date fixed effects to capture common time trends. We use two-way robust clustered standard errors at the city and date level. We restrict the sample period to six hours before sunset, the sunset hour, and four hours after sunset, from January 2015 to December 2017.

Coefficient β in Eq. (1) essentially captures the before-after difference of the average hourly increase in pollutants between the treatment and control stations. The identification assumption requires that the growth pattern of $P_{i,t}$ in the control stations is parallel to the ones in the treated stations before and after sunset if disguised pollution is absent. We test pre-trends in the next section. In addition to the hourly average difference, we also investigate the cumulative effect in the post-sunset hours using an event study design as follows:

$$P_{i,t} = \sum_{k \in \{-6,-5,-4,-3,-2,0,1,2,3,4\}} \beta_k \times T_{i,t} \times 1\{SunsetHour_{i,t} = k\} + \lambda \times W_{i,t} + \pi_k \times 1\{SunsetHour_{i,t} = k\} + \alpha_{i,r} + \mu_{c,h} + \delta_d + \varepsilon_{i,t} \tag{2}$$

where $1\{SunsetHour_{i,t} = k\}$ is a dummy variable that equals 1 if $SunsetHour_{i,t} = k$, otherwise 0. $SunsetHour_{i,t}$ refers to the hour relative to sunset time for station i, time t. In this event study, we use the pollution level one hour before sunset time as the benchmark period. The sample period is from six hours before sunset to four hours after sunset for each treatment and control station. The rest of the variables are defined the same as in Eq. (1).

Table 1
Summary statistics.

Panel A: Station Level								
	Bottom 20%				Top 20%			
	mean	sd	min	max	mean	sd	min	max
# of SO_2 factories	0	0	0	0	3.21	2.17	2	14
Sample size (# of stations)	310				119			
Panel B: Station-Hour Level								
	[-6, sunset)		[sunset, +4]		[-6, sunset)		[sunset, +4]	
	mean	sd	mean	sd	mean	sd	mean	sd
SO_2	19.58	31.66	18.11	29.59	21.21	33.68	20.17	30.52
Wind Speed (m/s)	30.01	19.01	23.41	16.55	33.06	19.74	27.15	19.49
Temperature (°C)	17.42	11.31	14.48	10.66	19.39	10.31	16.85	9.78
Dew Temperature (°C)	5.68	13.28	6.24	13.17	10.12	11.86	10.52	11.67
Precipitation (mm)	0.37	3.77	0.44	3.48	0.31	2.67	0.38	2.83
Wind Direction (8 h min, °)	127.11	95.87	130.75	97.84	116.83	92.97	117.50	91.68
Wind Direction (8 h max, °)	258.82	95.59	249.70	99.45	245.37	98.93	236.82	101.59
Boundary Layer Height (m)	1062.28	706.19	309.08	393.79	949.73	501.31	316.50	309.67
Surface Pressure (Pa)	92449.96	10783.29	92499.52	10768.31	99818.03	3463.54	99856.47	3456.18
Sample size	1,859,157		1,563,122		690,995		581,484	
Panel C: Firm Level (312 firms)								
	Key Region (263 firms)				Non-key Region (49 firms)			
	mean	sd	mean	sd	mean	sd	mean	sd
Compliance Rate	0.947	0.22	0.950	0.22	0.967	0.18	0.963	0.19
SO_2	77.01	190.01	76.32	164.04	86.76	177.76	87.65	179.42
Sample size	594,130		484,914		104,970		87,703	

NOTES: Panel A reports the average number of SO_2 factories within 3 km of each monitoring station at the bottom 20% and top 20%. Panel B reports the average pollutant readings before and after sunset for stations of the two groups. In the main regressions, the bottom 20% stations are the control group, while the top 20% stations are the treatment group. The sample period is from 2015 to 2017. Panel C reports the average of the hourly SO_2 and compliance rate before and after sunset for firms covered by the CEMS system. The sample period for firm analysis is 2015.

As another specification for robustness, we also use continuous treatment, namely the number of SO_2-producing firms within a given radius for each station i, to define the treatment intensity of station i. In the continuous treatment setting, we utilize the full sample of all stations to check the robustness of our results. The econometric specification is as follows:

$$P_{i,t} = \gamma Sunset_{i,t} \times Num_i + \delta Sunset_{i,t} + \lambda \times W_{i,t} + \alpha_{i,r} + \mu_{c,h} + \delta_d + \varepsilon_{i,t} \quad (3)$$

where Num_i is the number of SO_2 emitting firms within a given radius of station i, γ captures the marginal effect of one more nearby dirty factories on the SO_2 concentration level after sunset.

To examine firms' response around sunrise, we also conduct an event study for sunrise as follows:

$$P_{i,t} = \sum_{k \in \{-6,-5,-4,-3,-2,0,1,2,3,4\}} \beta_k \times T_{i,t} \times 1\{SunriseHour_{i,t} = k\} + \lambda \times W_{i,t} + \pi_k \times 1\{SunriseHour_{i,t} = k\} + \alpha_{i,r} + \mu_{c,h} + \delta_d + \varepsilon_{i,t} \quad (4)$$

where $1\{SunriseHour_{i,t} = k\}$ is a dummy variable that equals 1 if $SunriseHour_{i,t} = k$, otherwise 0. $SunriseHour_{i,t}$ refers to the hour relative to sunrise time for station i, time t. In this event study, we use the pollution level one hour before sunrise time as the benchmark period. The sample period is from six hours before sunrise to four hours after sunrise for each treatment and control station. The rest of the variables are defined the same as in Eq. (1).

For firm-level analysis, we adopt a single difference research design by comparing a firm's pollution behavior before and after sunset, conditional on high dimensional fixed effects as follows:

$$P_{i,t} = \eta Sunset_{i,t} + \lambda \times W_{i,t} + \alpha_{i,r} + \mu_d + \delta_h + \varepsilon_{i,t} \quad (5)$$

where $P_{i,t}$ denotes the SO_2 level (in log form) or the compliance dummy in firm-unit i, time t;$\alpha_{i,r}$ stands for firm-by-unit-by-year fixed effects; μ_d stands for date fixed effects; δ_h represents hour fixed effects. The rest of the notations are the same as in Eq. (1). In some specifications, we also interact $Sunset_{i,t}$ with a dummy variable indicating key regions monitored by the MEP to test the differential effects in key regions and other regions. Essentially, η captures the average change in $P_{i,t}$ after sunset, conditional on weather, firm-unit-year fixed effects, date fixed effects, and hour fixed effects. We use two-way robust clustered standard errors at the firm and date level. The sample period is the year 2015.

5. Main findings

Table 2 presents the main results for the station-level analysis using both the full sample and a restricted sample. In the main regressions, we define the treatment stations as those that are in the top 20% in terms of both the total number of factories and the number of factories in SO_2-intensive industries. We define the control stations as those that are in the bottom 20% for these two criteria. This definition results in 119 treatment stations and 310 control stations in 192 cities across China. Fig. 1 shows the spatial distribution of stations.

To preliminarily validate the comparability of our treatment and control groups, we first plot the raw trends of SO_2 (in log form) of the treatment and control groups before and after sunset, as shown in Fig. 2. We can see that the changes in pollution levels move parallel before sunset and start to deviate after sunset, even without any regression adjustment.

Table 2
Baseline – the effect of sunset on air pollution.

VARIABLES	(1) lnso2	(2) lnso2	(3) lnso2	(4) lnso2	(5) lnso2	(6) lnso2
Panel A: full sample						
Treat*Sunset	0.021	0.041***	0.054***	0.043*	0.066***	0.063***
	(0.015)	(0.015)	(0.016)	(0.022)	(0.019)	(0.018)
Observations	4,453,879	4,073,532	4,099,314	4,453,879	4,073,532	4,099,314
R-squared	0.437	0.463	0.469	0.459	0.482	0.487
Panel B: restricted sample (33 cities)						
Treat*Sunset	0.066***	0.067***	0.061***	0.060***	0.053***	0.051***
	(0.019)	(0.019)	(0.018)	(0.018)	(0.017)	(0.017)
Observations	1,177,169	1,134,821	1,144,133	1,177,169	1,134,821	1,144,133
R-squared	0.447	0.481	0.489	0.466	0.496	0.503
Atmospheric conditions		Yes (bin)	Yes (poly)		Yes (bin)	Yes (poly)
Date FE	Yes	Yes	Yes	Yes	Yes	Yes
Station-Year FE	Yes	Yes	Yes	Yes	Yes	Yes
City-Hour FE				Yes	Yes	Yes
Cluster	city date	city date	city date	city date	city date	city date

NOTES: This table reports the regression results using the full sample in Panel A and the restricted sample in Panel B. Atmospheric conditions include precipitation, wind speed, wind direction, temperature, dew point, daily range of temperature, boundary layer height, and surface pressure. Standard errors are robustly two-way clustered at city and date levels. *P < 0.10;**P < 0.05;***P < 0.01. The sample period is 2015–2017.

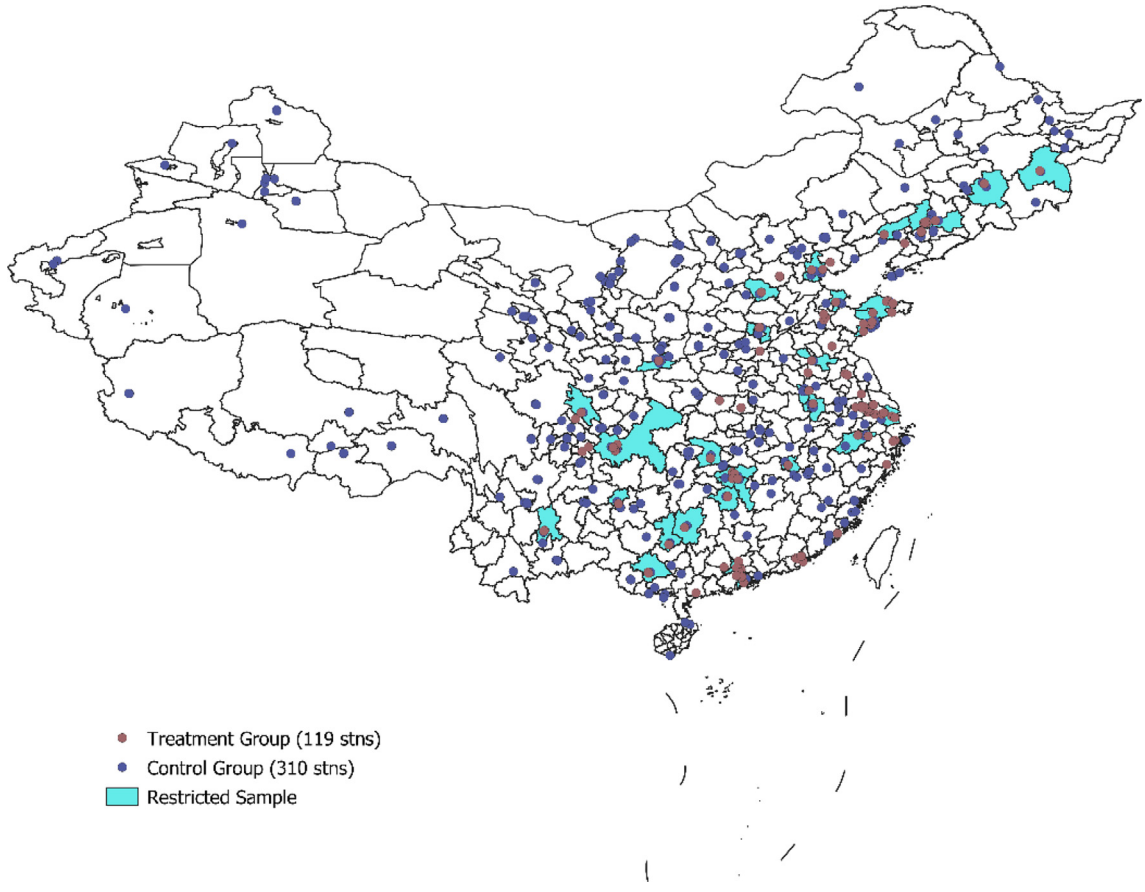

Fig. 1. Distribution of treatment and control stations (full and restricted sample). We plot the distribution of monitoring stations in the control group and the treatment group in this map. In the full sample, there are 119 treatment stations and 310 control stations in 192 cities across China. In the restricted sample represented by the cyan areas, there are 57 treatment stations and 60 control stations in 33 cities. (For interpretation of the references to color in this figure legend, the reader is referred to the web version of this article.)

Table 2 Panel A presents our main analyses using the full sample. The analyses emphasize the importance of controlling city-hour fixed effects and atmospheric conditions when using the full sample. First, city-hour fixed effects allow us to utilize the variation within a city-hour cell. To capture transportation policy shifts and electricity price changes, city-hour fixed effects are necessary, especially for the full sample that covers a wide geographical area. Columns 1 to 3 and columns 4 to 6 show the results without and with controlling city-hour fixed effects, respectively. We can observe from columns 4 to 6 in Panel A that the estimates are relatively stable across different specifications after controlling for city-hour fixed effects.

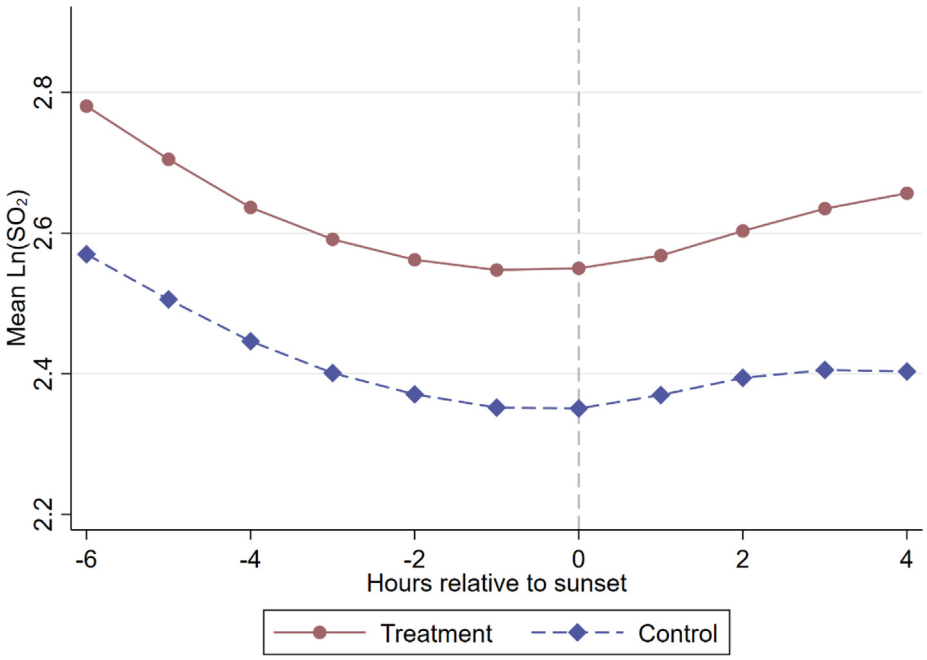

Fig. 2. The raw trend of ln(SO_2) in the treatment and control groups. The figure presents the average level of ln(SO_2) aggregated by the treatment stations and control stations six hours before and four hours after sunset without any regression adjustments.

Second, the transmission and diffusion of pollutants are related to atmospheric conditions such as wind speed and temperature. To capture the atmospheric changes after sunset as much as possible, we flexibly controlled the bins (column 5) or polynomial forms (column 6) of atmospheric conditions (wind direction, wind speed, temperature, dew point temperature, daily range of temperature, precipitation, surface pressure, and boundary layer height), under the assumption that the treatment group and control group in our sample are comparable conditional on these atmospheric controls. We obtain positive estimates from different specifications of atmospheric controls. Since city-hour fixed effects are essential, we mainly look at columns 4 to 6. In particular, compared with columns 5 and 6, the estimates in column 4 that did not control atmospheric conditions are biased, although remain positive (significant at 10% level).

Nevertheless, in some cities, we may have either treatment stations or control stations but not both. To ensure better comparability between the two groups, we further restrict our sample to cities that contain at least one treatment station and one control station. The refined sample results in 57 treatment stations and 60 control stations in 33 cities (see the cyan polygons in Fig. 1). We replicate our main analyses in Table 2 Panel B, which are largely consistent with the results in Table 2 Panel A using the full sample. The effect is 1.2% smaller in magnitude using the restricted sample (as shown in column 6 of Panel B).

The results in Table 2 Panel B further confirm the credibility of the restricted sample. We can see that estimates across columns 1 and 6 in Panel B are similar, whether controlling for city-hour fixed effects and atmospheric conditions or not. The high consistency in the estimates across all specifications in Panel B reflects the credibility of the restricted sample and that the treatment and control groups are highly comparable in the restricted sample, even when not conditional on atmospheric conditions.

Overall, considering the size and geographical coverage of the sample, we use the full sample, absorb city-hour fixed effects and flexibly control for atmospheric conditions. Therefore, we prefer column 6 to be the baseline results. As shown in column 6 of Table 2, SO_2 is increased by 6.3% per hour after sunset in the treated stations, which is significant at the 1% level. We further conduct robustness checks in Section 5.2 to rule out alternative stories such as atmospheric phenomena or electricity generation. In addition, as discussed before, SO_2 is a primary rather than a secondary pollutant, so we are confident that the increase in SO_2 is caused by industrial emissions after sunset.

5.1. Comparability of the treatment and control group

Our identification strategy relies heavily on the comparability of the treatment and control groups. In this subsection, we test this assumption from various perspectives. We previously compared the raw time trends of SO_2 (in log form) between the treatment and control groups as shown in Fig. 2. Then, to test if the observable meteorological conditions could differ across areas before and after sunset and thus further verify whether the treatment and control groups are comparable, we use our primary difference-in-differences model but replace the dependent variable with each weather control in the following analysis. Table 3 reports the estimated coefficients of two core independent variables, Sunset and Treat*Sunset, respectively. Conditional on the same set of fixed effects as the main specification, the coefficients of Sunset are statistically significant, except for the result for surface pressure, indicating that atmospheric conditions do indeed change after sunset. Consistent with the findings in environmental science literature, many indicators suggest worse diffusion conditions after sunset. For example, the wind speed and boundary layer height (BLH) drop considerably, leading to the accumulation of pollutants at the ground level. However, as shown in Table 3 Panel A, the coefficients of Treat*Sunset show that most weather conditions (temperature, dew point temperature, precipitation, wind speed, and wind direction) do not change differently between treatment and control groups after sunset. The only two exceptions that move differently between these two groups are boundary layer height and surface pressure. Specifically, the regression results suggest that both surface pressure and BLH have a smaller decrement in the treatment areas than in control areas. However, the relative values of the decrement for surface pressure and BLH are very small compared to their mean values. More importantly, since high surface pressure and high boundary layer height have both been widely

Table 3
Atmospheric conditions of treatment and control groups.

VARIABLES	(1) Temperature	(2) Wind speed	(3) Dew temperature	(4) Rain	(5) Wind direction	(6) Surface pressure	(7) BLH
Panel A: full sample							
Sunset	−1.758***	−1.078***	−1.392***	0.293***	2.451***	−10.351	−177.640***
	(0.161)	(0.196)	(0.139)	(0.033)	(0.906)	(12.723)	(15.615)
Treat*Sunset	0.286	−0.059	0.031	−0.008	0.721	117.260***	55.836***
	(0.230)	(0.197)	(0.222)	(0.024)	(1.175)	(21.404)	(17.507)
Observations	4,669,208	4,669,517	4,668,020	4,669,284	4,667,302	4,694,757	4,694,757
R-squared	0.853	0.327	0.876	0.144	0.180	0.998	0.543
Benchmark	16.660	27.912	7.117	0.387	251.075	94468.284	702.566
Relative Value	0.017	−0.002	0.004	−0.022	0.003	0.001	0.079
Panel B: restricted sample							
Sunset	−1.439***	−0.926**	−1.534***	0.238***	2.746**	52.834***	−67.626***
	(0.280)	(0.424)	(0.234)	(0.030)	(1.329)	(18.683)	(15.364)
Treat*Sunset	−0.081	−0.128	−0.043	0.012	−0.410	−8.008*	−16.080
	(0.084)	(0.168)	(0.103)	(0.015)	(0.996)	(4.034)	(13.347)
Observations	1,243,672	1,244,618	1,243,299	1,243,672	1,244,533	1,254,936	1,254,936
R-squared	0.863	0.325	0.870	0.084	0.213	0.994	0.537
Benchmark	17.720	30.516	9.400	0.313	254.882	99084.815	647.458
Relative Value	−0.005	−0.004	−0.005	0.037	−0.002	−0.0001	−0.025
Date FE	Yes	Yes	Yes	Yes	Yes	Yes	Yes
Station-Year FE	Yes	Yes	Yes	Yes	Yes	Yes	Yes
City-Hour FE	Yes	Yes	Yes	Yes	Yes	Yes	Yes
Cluster	city date	city date	city date	city date	city date	city date	city date

NOTES: This table reports the coefficients of Sunset and Treat*Sunset, following our main specification but replacing the dependent variable with the respective atmospheric control. The relative value is the ratio between the coefficient of Treat*Sunset and the mean value of the dependent variable. The time period is from 2015 to 2017. Standard errors are robustly two-way clustered at city and date levels. *P < 0.10;**P < 0.05;***P < 0.01.

shown to be conducive to the diffusion of pollutants (Xiang et al., 2019), our estimates should be at least at the lower bounds of the disguised pollution. In addition, compared to Table 3 Panel A, the results in Panel B using the restricted sample show that there are negligible differences for all weather conditions; in other words, the treatment group and control group are highly comparable in this regard. Although the coefficient of Treat*Sunset for surface pressure is marginally significant, the relative magnitude is extremely small compared to the mean value of surface pressure.

Third, Fig. 3 presents the event study on SO_2 (in log form, regression results available in Table A3). The coefficients represent the difference in the pollution level in a certain hour (relative to the sunset hour) compared to the first hour before sunset. Therefore, the coefficient captures the cumulative effect of disguised pollution after sunset. As shown in Fig. 3, SO_2 significantly increases after the sunset hour. The overall SO_2 level increases by 10.8% until four hours after sunset compared to before sunset. In absolute terms, the event study suggests that the SO_2 increased by 2.58 $\mu g/m^3$ four hours after sunset using the pre-sunset 6-hour average (in the treatment group) as the baseline.

The event study helps us to look at the pre-trends. In the six hours before sunset, the changes in pollutant levels between the treatment and control groups are not jointly significantly different. However, the coefficients at hour = −2 and −3 are statistically significant (although economically insignificant) at the 5% level. According to the literature and its associated programming package, the sunset time utilized in our study is calculated mechanically based on three crucial variables; latitude, longitude, and date (Corripio, 2003). However, apart from these three key determinants, there are other potential factors, such as elevation, that could also affect visibility around sunset time, which could cause a measurement error of the exact time at which the discharged smoke is no longer visible to the naked eye. There are two reasons why elevation affects visibility around sunset time. First, due to the phenomenon of refraction of light, locations at higher elevations usually observe sunset later than those at lower elevations, even if the latitudes and longitudes of these locations are identical. Second, the topography can also affect how much light is seen; that is, areas surrounded by mountains may have poorer visibility conditions.

To further illustrate how the composition of stations at different altitudes affects the performance of the parallel pre-trend test, we use 1,000 m as a threshold of elevation and divide the full sample into low- and high-elevation groups, which comprises 116 (3) treatment stations and 213 (97) control stations, respectively. As shown in the event study in Fig. A4, the DID coefficients prior to sunset estimated using only low-altitude stations (elevation<1,000 m) are not significantly different from zero both individually and jointly, and no significantly different pre-trend can be visually observed.

In addition, in the event study results of the restricted sample shown in Appendix Fig. A5, the pre-sunset coefficients are individually and jointly statistically insignificant, which further give us confidence in the previous statement that the treatment and control groups are highly comparable in the restricted sample.

Lastly, we explore how well-powered this test is in our context, although we do not find evidence of differential pre-trends in the event study. Following Roth (2022), we first determine the size of a linear pre-trend we are able to detect. As shown in Fig. 4, our analysis suggests that we could detect a small positive linear trend of a magnitude of 0.00899 or greater (in absolute terms) with 80% power in our event study (i.e., we have an 80% probability of finding a significant pre-trend under the pre-trend of such size). If a trend of a size of up to 0.00899 is indeed present (although not detectable to us), we calculate that it would generate a bias of at most 0.03525 by post-hour 4 following the expansion. Our actual estimate in post-hour 4 is 0.1079 and is substantially larger (3.06 ×) than this potential bias.

5.2. Robustness checks

In this subsection, we conduct a few robustness checks. We show that our estimated effect is not driven by the alternative stories of atmospheric phenomena, electricity demand, normal production shifts, coal-burning for heating purposes, and traffic flow changes, but is because of firm emission behaviors.

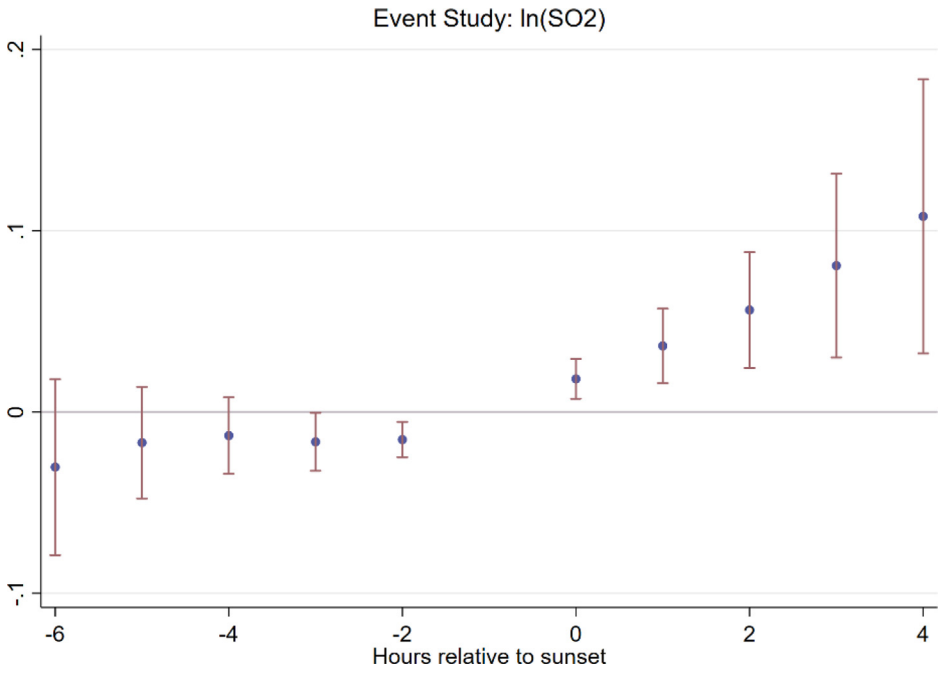

Fig. 3. Event study (sunset). This figure presents the coefficients and 95% confidence interval of the event study. The event time is the sunset hour. The baseline average is the first hour before sunset. The coefficient estimates are available in Table A3.

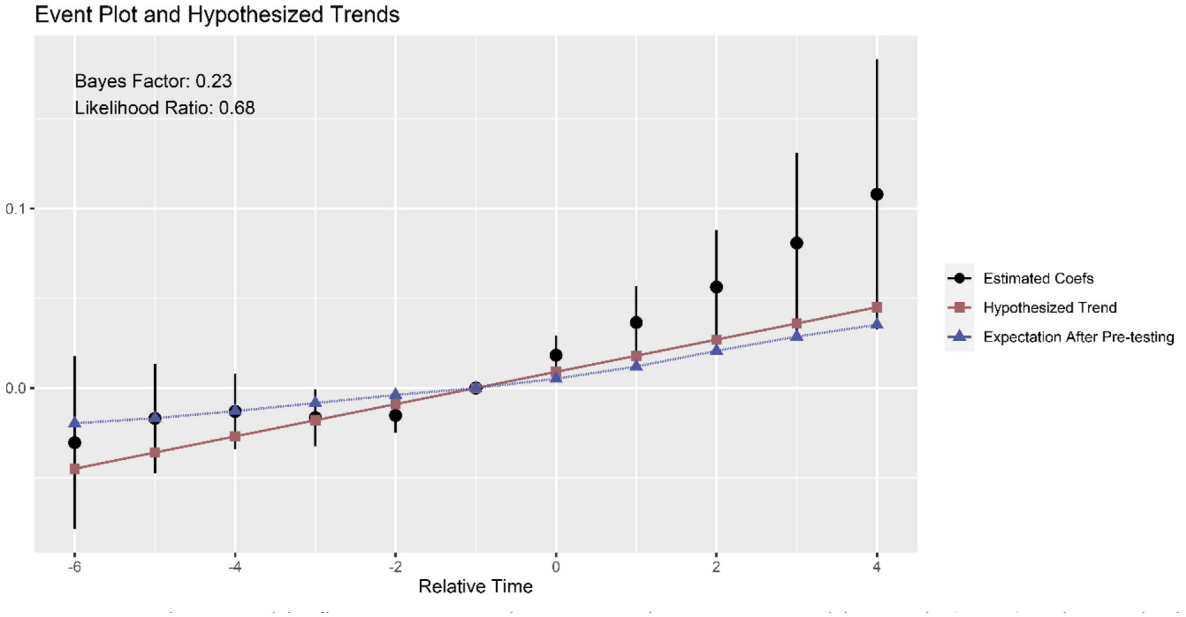

Fig. 4. Pre-trends test. This figure presents the pre-trends test proposed by Roth (2022). The analysis suggests that we can detect a fairly small positive linear trend of a magnitude of 0.00899 (the slope of the red line) or greater (in absolute terms) with 80% power in our event study. If a trend of a size of up to 0.00899 is indeed present, we calculate that it would generate a bias of at most 0.03525 by post hour 4 following the expansion, as shown by the blue line. (For interpretation of the references to color in this figure legend, the reader is referred to the web version of this article.)

Atmospheric changes. Generally, the diurnal variations of pollutants exhibiting an early morning peak and a small secondary peak in the evening are well documented in the literature. One may worry that the disguised pollution we find is a kind of atmospheric phenomenon instead of being due to firms' behavior. Studies in environmental science report that dissipation (meteorological) and emission rate (anthropogenic) are the two main sources of the diurnal variation in pollution (Halliday and Kemeny, 1964; Kuerban et al., 2020; Raynor et al., 1974; Zhang and Cao, 2015). We acknowledge that the changes in meteorological conditions, including temperature, relative humidity, wind, precipitation, surface pressure, and boundary layer height, may negatively influence the dissipation rate of pollutants after sunset. However, we conduct our analyses under a difference-in-differences identification setting. Considering that the changes in meteorological conditions that occur in the treatment group and control group move in the same direction simultaneously (as presented in Table 3), the causal inferences of firms' polluting behavior should not be threatened.

Furthermore, we conduct additional tests, shown in Table 4. As with the results presented in Table 3, we find boundary layer height and surface pressure change are slightly different (although

Table 4
Robustness – control atmospheric conditions differently.

VARIABLES	(1) lnso2	(2) lnso2	(3) lnso2	(4) lnso2
Panel A: full sample				
Treat*Sunset	0.057***	0.063***	0.063***	0.064***
	(0.020)	(0.018)	(0.019)	(0.018)
Observations	4,099,314	4,099,314	4,096,299	4,099,314
R-squared	0.482	0.487	0.487	0.488
Panel B: restricted sample (33 cities)				
Treat*Sunset	0.055***	0.051***	0.054***	0.051***
	(0.017)	(0.017)	(0.017)	(0.017)
Observations	1,144,133	1,144,133	1,143,363	1,144,133
R-squared	0.499	0.503	0.503	0.505
Weather	Yes	Yes	Yes	Yes
BLH & SP		Yes		Yes
pre-sunset BLH & SP			Yes	
weather interactions				Yes
Date FE	Yes	Yes	Yes	Yes
Station-Year FE	Yes	Yes	Yes	Yes
City-Hour FE	Yes	Yes	Yes	Yes
Cluster	city date	city date	city date	city date

NOTES: This table reports the regression results using different specifications in terms of atmospheric conditions. Column 1 does not include boundary layer height (BLH) and surface pressure (SP) as controls; column 2 is our baseline specification, which controls BLH and SP; column 3 controls the average pre-sunset BLH and SP; column 4 adds the interactions of temperature with wind speed, temperature with precipitation, wind direction with wind speed, and wind speed with precipitation, based on column 2. The time period is from 2015 to 2017. Standard errors are robustly two-way clustered at city and date levels. *P < 0.10;**P < 0.05;***P < 0.01.

in a small magnitude) between the treatment and control group after sunset, which may indicate these two variables are 'bad controls'. Therefore, we conduct robustness checks by excluding these two controls (column 1), and controlling the average *pre-sunset* boundary layer height and surface pressure (column 3), respectively. Compared with our baseline results in Table 4 column 2 (also Table 2 column 6), the estimates using different specifications in terms of boundary layer height and surface pressure are similar. We also flexibly control for atmospheric conditions by adding interactions of temperature with wind speed, temperature with precipitation, wind direction with wind speed, and wind speed with precipitation, and still, the results are similar.

Electricity generation and electricity price. We exclude the alternative story of electricity demand change after sunset based on the results presented in Table 5. One story related to electricity is that powerplants may need to produce more electricity to meet the peak demand after sunset, thus driving up pollution after sunset. To deal with this concern, we exclude treated stations from our sample if there are any powerplants within a 3 km radius, which reduces the number of stations by 34. The regression results remain similar to Table 2, as presented in Table 5 column 1. We further add city-relative (-to-sunset)-hour fixed effects, to capture electricity demand changes right after sunset, and the results in columns 2 and 3 remain similar to our baseline.

The other story related to electricity is that firms may produce during the night shift because the electricity price may be cheaper at night. In this case, the increase in pollution after sunset is not a disguised behavior, but a reflection of firms' shift of production from daytime to nighttime. As for this story, first, electricity price changes are by the hour instead of by sunset, which is absorbed in the city-hour fixed effects. In addition, we manually collect the electricity price data for each province. As shown in Appendix Fig. A6, the electricity price is generally higher in the first few hours after sunset (the average sunset hour in our sample is approximately 6:32 pm). Therefore, firms should reduce their production after sunset if they want to save on electricity costs. For alternative tests, we restrict the sample in two ways: 1) we restrict to cities where the average electricity price six hours before sunset is lower than the average electricity price four hours after sunset, and thus drop approximately 17% of the observations; 2) we restrict to cities where the average electricity price six hours before sunset is equal to the average electricity price four hours after sunset, and thus keep only 10% of the observations. In these two restricted samples, firms should not have an incentive to shift production from daytime to post-sunset to save electricity costs. As shown in Table 5 columns 4 and 5, the estimated coefficients are still significantly positive, and the magnitude is even slightly larger in column 5, suggesting that our results are not driven by the change in electricity prices.

Industrial production changes corresponding with nightfall. One could plausibly voice a concern that the rising pollution gap between the industrial and non-industrial areas does not necessarily reflect firms' strategic responses to pollution monitoring and regulation enforcement, but reflects normal shifts in economic activities that correspond with nightfall, such as nocturnal manufacturing operations. We rule out this alternative story based on the following three points.

First, for an average industrial firm, the production costs that may vary with time within a day typically include labor costs, electricity costs, and, in the context of this paper, desulfurization costs. Among these costs, labor costs usually increase during nighttime because of overtime pay or night shift differential pay; besides, electricity costs are also higher during this time.[15] Therefore, theoretically, a firm would not have an incentive to expand production after sunset considering the increased costs of labor and electricity. Instead, the relative increase in SO_2 in the industrial areas after sunset is more likely to be the consequence of firms turning off the scrubbers to reduce desulfurization costs.

Second, according to the technical requirements for environmental protection products released by Ministry of Ecology and Environment of China, the desulfurization efficiency of the desulfurization equipment should be greater than 80%.[16] Even if all of the

[15] As shown in Fig. A.6, most of the peak electricity prices occur at 7pm, which is approximately one or two hours after sunset.

[16] Please refer to https://www.mee.gov.cn/ywgz/fgbz/bz/bzwb/other/hbcpjsyq/200607/W020111221562339416293.pdf (accessed on March 9, 2023). The specifications for environmental protection product (Wet flue-gas desulphurization and precipitator device) stipulates the desulfurization efficiency of the desulfurization and dust removal devices utilizing chemical desulfurization machines to reduce the concentration of sulfur dioxide emissions in flue gas should exceed 80%.

Table 5
Electricity demand and electricity price.

	(1) lnso2	(2) lnso2	(3) lnso2	(4) lnso2	(5) lnso2
	electricity generation			electricity price	
Treat*Sunset	0.071***	0.046***	0.046***	0.053***	0.078***
	(0.019)	(0.015)	(0.016)	(0.017)	(0.015)
Observations	3,769,166	4,099,314	4,099,314	3,417,647	395,843
R-squared	0.485	0.479	0.518	0.487	0.489
Sample	Exclude powerplant	all	all	P_{mean}(after) > P_{mean}(before)	P_{mean}(after) = P_{mean}(before)
Atmospheric conditions	Yes	Yes	Yes	Yes	Yes
Date FE	Yes	Yes	Yes	Yes	Yes
Station-Year FE	Yes	Yes	Yes	Yes	Yes
City-Hour FE	Yes		Yes	Yes	Yes
City-Relative-Hour FE		Yes	Yes		
Cluster	city date	city date	city date	city date	city date

NOTES: This table rules out alternative stories related to electricity demand. Column 1 excludes treated stations from our sample if there are any power plants within a 3 km radius. Columns 2 and 3 control city-relative-hour fixed effects to absorb the electricity demand change relative to sunset. Column 4 restricts the sample to cities where the minimum electricity price six hours before sunset is lower than the minimum electricity price four hours after sunset, and column 5 restricts the sample to cities where the average electricity price six hours before sunset is equal to the average electricity price four hours after sunset. The time period is from 2015 to 2017. Standard errors are robustly two-way clustered at city and date levels. *P < 0.10;**P < 0.05;***P < 0.01.

firms increase their production rate by 5% after sunset, SO_2 would increase by at most 1% (=5%*(1–80%)), which is much less than the magnitude of SO_2 increment that we have shown. To achieve the observed 6.3% increase in SO_2, every firm's production would have to increase substantially by at least 31.5% (=6.3%/(1–80%)) after sunset. In other words, it is not realistic to find an impact as large as a 6.3% increase in SO_2 after sunset if all firms increase production and keep the desulfurization equipment running.

Third, we attempt to empirically infer changes in the production activities of firms using CEMS data. In the CEMS data of Zhejiang Province, 34 firms report flue gas flow or the rate of flue gas flow, which could act as proxies for the hourly production output. Table A4 shows the comparisons of flue gas flow and flue gas flow rate before and after sunset for a subsample of the CEMS firms in Zhejiang Province. The coefficients on the sunset variable are statistically insignificant, implying that firms' production does not significantly increase after sunset.[17]

Winter heating and traffic flows. Fourth, we rule out the possibility that increases in SO_2 are driven by heating and traffic flow changes after sunset. Residents near the treated stations burn more coal for heating purposes after sunset than the control stations. Coal-burning by residents is common in China, especially in rural and suburban areas. The coal used by local residents may produce SO_2 due to incomplete combustion. After sunset, the temperature drops, which may increase coal-burning activities. Moreover, the coal-burning activities may increase more after sunset near the treated monitoring stations than the control stations because the population density (for example, housing for workers of the surrounding factories) near treated stations may be higher than the control stations. In Table 6, we show that the above story is unlikely to explain our findings. As presented in Table 6 column 1, the results remain similar to Table 2 if we exclude the whole winter heating season from the sample (November to March) for all the stations. In Table 6 column 2, we interact temperature with the DID term. In column 3, we define a variable "NeedHeating" that equals 1 if the temperature is below 10 degrees Celsius, otherwise 0. We interact "NeedHeating" with the DID term, and the triple difference term Treat*Sunset*Temperature. We also control for all the pairwise and triple difference interactions. Even though our treatment effect decreases with temperature, we do not find that the treatment effect correlates with temperature during the heating season (when the temperature is below 10 degrees Celsius).

Another possible story is that the increase in pollution after sunset is driven by vehicles instead of factory emissions. There might be more diesel trucks at night because diesel trucks are generally not allowed to enter the main roads in major cities in the daytime, thus producing more SO_2 after sunset. However, our results are not likely to be driven by diesel trucks for two reasons. First, the entry restriction on trucks is by the hour instead of by sunset time. For example, trucks cannot enter the major urban area in Beijing before midnight (12 am) and after 6 am. Therefore, the policy shift is already captured by the city-hour fixed effects. In addition, to further reassure readers that our results are not confounded by policy changes on trucks, we measure the major road length (in km) within a 3 km radius of each monitoring station and interact the road length with the DID coefficient. The heterogeneity analysis suggests that the disguised pollution effect is almost the same in monitoring stations with more dense road networks, as presented in Table 6 column 4. We conduct two additional tests by 1) excluding the city-day observations if trucks are allowed to enter the major urban area in our post-event window (i.e., within four hours post-sunset), and 2) excluding the post-sunset hours that trucks are allowed to enter the major urban area (i.e., drop the hours affected instead of all the hours in that city-day cell). The results are reported in Appendix Table A1 with an even larger magnitude for the estimation of SO_2.

Define different treatment variables. Lastly, we conduct analyses using continuous treatment, which is defined as the number of SO_2 factories within various radii of each station instead of a dummy variable. In this way, the regressions in Table 7 use data from all stations, and the coefficient of the core interaction term "NumOfFirms*Sunset" represents the marginal effect of one more nearby dirty factories on the SO_2 concentration level after sunset. As we can see in Table 7, the coefficients for different radii are statistically significant, which is consistent with our main finding. We also change the radii that are used to define the treatment group into 4 km or 5 km and find our findings remain similar, as shown in Appendix Table A2.

[17] Nevertheless, we admit that there is a lack of clear quantified relationship between the production rate and the flue gas flow rate monitored by the CEMS. In addition, these two metrics are related to a series of other factors including atmospheric pressure, static flue gas pressure, flue gas temperature, and moisture content in the flue gas. More importantly, the CEMS data in China currently only cover some of the largest industrial firms and not all of the CEMS firms have reported information of flue gas flow and the rate of flue gas flow. Therefore, the sample used in the regressions is hardly representative of all the industrial firms in China, thus the findings based on these tests are only suggestive.

Table 6
Robustness – temperature, winter heating, and road network.

VARIABLES	(1) lnso2	(2) lnso2	(3) lnso2	(4) lnso2
	exclude Nov-March			
Treat*AftSun	0.037**	0.050*	0.040	0.076**
	(0.015)	(0.029)	(0.025)	(0.035)
Treat*AftSun*Temperature		−0.001	−0.0004	
		(0.002)	(0.001)	
Treat*AftSun*NeedHeating			0.014	
			(0.034)	
Treat*AftSun*Temperature*NeedHeating			−0.003	
			(0.005)	
Treat*AftSun*Roadkm				−0.0002
				(0.0004)
Observations	2,377,166	4,099,314	4,099,314	4,066,091
R-squared	0.434	0.487	0.489	0.481
Atmospheric conditions	Yes	Yes	Yes	Yes
Date FE	Yes	Yes	Yes	Yes
Station-Year FE	Yes	Yes	Yes	Yes
City-Hour FE	Yes	Yes	Yes	Yes
Cluster	city date	city date	city date	city date

NOTES: This table rules out the alternative hypothesis that our observed effect is driven by residents burning coal for heating purposes or driven by the change in traffic flows. Column 1 replicates Table 2 in the paper, excluding the winter heating period (November to March). In columns 2 and 3, we interact temperature with the DID term. Moreover, we define a variable "NeedHeating" that equals 1 if the temperature is below 10 Celsius degrees, otherwise 0. We interact "NeedHeating" with the DID term, and the triple difference term Treat*Sunset* Temperature. We also control for all the pairwise and triple difference interactions. In column 4, we add the interaction of road length with the DID term. All columns use 429 monitoring stations in 192 cities. The time period is from 2015 to 2017. Standard errors are robustly two-way clustered at city and day levels. *P < 0.10;**P < 0.05;***P < 0.01.

Table 7
Robustness – continuous treatment.

VARIABLES	(1) lnso2	(2) lnso2	(3) lnso2	(4) lnso2	(5) lnso2	(6) lnso2	(7) lnso2	(8) lnso2
NumOfFirms*Sunset	0.005*	0.004*	0.005**	0.005***	0.004**	0.003**	0.004**	0.004**
	(0.003)	(0.002)	(0.002)	(0.002)	(0.002)	(0.001)	(0.001)	(0.001)
Observations	12,654,383	12,654,383	12,654,383	12,654,383	12,654,383	12,654,383	12,654,383	12,654,383
R-squared	0.490	0.490	0.490	0.490	0.490	0.490	0.490	0.490
Radius	3 km	4 km	5 km	6 km	7 km	8 km	9 km	10 km
Weather	Yes	Yes	Yes	Yes	Yes	Yes	Yes	Yes
Date FE	Yes	Yes	Yes	Yes	Yes	Yes	Yes	Yes
Station-Year FE	Yes	Yes	Yes	Yes	Yes	Yes	Yes	Yes
City-Hour FE	Yes	Yes	Yes	Yes	Yes	Yes	Yes	Yes
Cluster	city date	city date	city date	city date	city date	city date	city date	city date

NOTES: This table reports the regression coefficients using Eq. (3). The treatment intensity (denoted by Num) is defined as the number of SO_2 firms within a given radius of the station. From columns 1 to 8, we set different radii from 3 km to 10 km. The time period is from 2015 to 2017. Standard errors are robustly two-way clustered at city and date levels. *P < 0.10;**P < 0.05;***P < 0.01.

6. Discussion

6.1. Disguised pollution and political factors

In this subsection, we further investigate the correlation between disguised pollution and economic growth pressure, political turnover, and central inspections. The following analyses indirectly verify that the effect documented in our paper is due to firms' emission behaviors instead of atmospheric chemical effects, which should not vary due to economic and political factors.

6.1.1. Political turnover

Officials face many challenges in areas such as economic growth and environmental governance, in part because they may lack of local knowledge when they are transferred to a new place (Shi et al., 2021). In this case, the new prefectural leader may not be able to take care of everything in his/her early days in office, especially behaviors disguised by night. Therefore, we expect the disguised pollution phenomenon to be more prominent in the early days when the new leader has just taken office. We conduct a triple-difference estimation and interact the DD term ($Sunset_{i,t} \times T_i$) with time dummies indicating periods within 0–5 months ($Turnover[0, 6m)$), within 6–11 months ($Turnover[6, 12m)$), and more than or equal to 12 months ($Turnover[12m, .)$) of the turnover of the prefectural leader, respectively. We also include all the pairwise terms but only report the coefficients relevant to our study.

Table 8 presents the correlation between political turnover and disguised pollution. Columns 1 and 3 only keep the 124 cities that experienced one turnover of the municipal party secretary during the sample period 2015–2017, and columns 2 and 4 keep the 180 cities that did not experience any or experienced one change of party secretary. As shown in Table 8, we find that in cities that experienced political turnover once during 2015–2017, the disguised pollution effect is 54.0%–61.9% (0.039/0.063 = 61.9%; 0.034/0.063 = 54.0%) higher half a year after the change of municipal party secretary, compared with periods before the political turnover.

Additionally, we investigate whether having experience related to environmental governance helps the leader overcome the disadvantage due to lack of local knowledge. As presented in columns 3 and 4, we find the turnover effect that increases disguised pollu-

Table 8
Political turnover and disguised pollution.

VARIABLES	(1) lnso2	(2) lnso2	(3) lnso2	(4) lnso2	(5) lnso2	(6) lnso2
	Party secretary				Mayor	
Treat*Sunset	0.033	0.037**	0.025	0.032*	0.039*	0.039**
	(0.020)	(0.018)	(0.020)	(0.018)	(0.020)	(0.018)
Treat*Sunset*Turnover [0,6m)	0.039***	0.034**	0.044***	0.037**	0.012	0.009
	(0.015)	(0.016)	(0.015)	(0.016)	(0.015)	(0.016)
Treat*Sunset*Turnover [6,12 m)	0.007	−0.001	0.012	0.002	0.004	0.0002
	(0.015)	(0.017)	(0.015)	(0.017)	(0.017)	(0.018)
Treat*Sunset*Turnover [12 m,.)	0.019	0.012	0.023	0.013	−0.009	−0.012
	(0.021)	(0.021)	(0.021)	(0.021)	(0.018)	(0.019)
Treat*Sunset*Turnover [0,6m)*Env			−0.145***	−0.139***		
			(0.029)	(0.030)		
Treat*Sunset*Turnover [6,12 m)*Env			−0.151**	−0.141*		
			(0.074)	(0.073)		
Treat*Sunset*Turnover [12 m,.)*Env			−0.073	−0.060		
			(0.069)	(0.071)		
Observations	2,323,031	3,297,384	2,323,031	3,297,384	2,429,595	3,097,414
R-squared	0.492	0.478	0.492	0.478	0.463	0.466
Sample	turnover = 1	turnover = 0–1	turnover = 1	turnover = 0–1	turnover = 1	turnover = 0–1
Atmospheric conditions	Yes	Yes	Yes	Yes	Yes	Yes
Date FE	Yes	Yes	Yes	Yes	Yes	Yes
Station-Year FE	Yes	Yes	Yes	Yes	Yes	Yes
City-Hour FE	Yes	Yes	Yes	Yes	Yes	Yes
Cluster	city date	city date	city date	city date	city date	city date

NOTES: This table reports the heterogeneity analysis by interacting the DID term with time dummies indicating periods within 0–5 months ($Turnover[0,6m)$), within 6–11 months ($Turnover[6,12m)$), and more than or equal to 12 months ($Turnover[12m,.)$) of the turnover of the prefectural leader, respectively. Columns 1–4 report the correlation between disguised pollution and the turnover of the party secretary, and columns 5–6 report the correlation with the turnover of the mayor. "*Env*" is a dummy equal to 1 if the leader has environmental governance experience, otherwise 0. Columns 1 and 3 only keep the 124 cities that experienced one turnover of the municipal party secretary during the sample period 2015–2017, and columns 2 and 4 keep the 180 cities that did not experience or experienced one change of party secretary. Same with columns 5 and 6.

tion in the first six months of the new secretary's tenure is significantly less noticeable if the new party secretary has environmental governance experience, relative to the party secretaries without environmental governance experience.

We did not find similar evidence in terms of mayoral change, which is probably because the party secretary plays a major role in the governance of a city in China and the promotion criteria for the secretary and mayor may also be different (Zuo, 2015). The correlation between disguised pollution and political turnover confirms that our finding is not a purely atmospheric phenomenon but is attributable to the emission behaviors of firms.

6.1.2. The role of inspections

We have shown above that firms pollute more after sunset to circumvent environmental regulations. In this section, we evaluate whether or not government inspections are effective in reducing firms' disguised pollution behavior. We exploit the staggered nationwide inspection on industrial pollution conducted by the MEP across all the provinces in China from December 2015 to August 2017. The inspection teams stayed in each province for one month to investigate pollution issues in that province. During their stay, the inspection team sets up hotlines and mailboxes and welcomes complaints about pollution-related issues. Complaints related to disguised pollution at night have been documented by the MEP inspection team as a type of representative case.[18] Fig. A7 presents the timeline for the central inspection of different provinces. From December 2015 to September 2017, the central inspectors conducted approximately five rounds of inspections. Each round typically covered 7–8 provinces simultaneously, with the exception of the first round, which only inspected Hebei province. The inspection team usually spent about a month (4.4 weeks on average) in each province.

We collect the exact start and end dates of the inspection teams in each province and investigate the dynamic effects at the weekly level during the inspection. We first conduct the analysis from a short-term perspective, restricting the periods from eight weeks before the inspection, five weeks during the inspection, and four weeks after the inspection as our sample. For each given date, certain provinces are inspected while others are not, allowing us to compare the pre- and post-sunset difference in treatment and control in the inspected provinces, with the pre- and post-sunset difference in treatment and control in non-inspected provinces. Fig. 5 shows the event study estimates of $Treat \times Sunset \times Inspect_t$, with coefficients reported in column 3 of Appendix Table A5. The coefficients in Fig. 5 represent the trend of disguised pollution behavior during and after the central government's inspection, compared to the benchmark period — eight to three weeks before the inspection. Our findings suggest that inspection may temporarily have a negative correlation with disguised pollution, with only the coefficients for the fourth week of the inspection showing marginal statistical significance (p-value of 0.08), while the coefficients for the other weeks are not statistically significant.[19] However, when the inspection team is about to leave, there is no significant difference in the disguised emission behavior after sunset compared to the benchmark period. Our findings are also in line with Karplus and Wu (2019), who find inspec-

[18] For example, Case 3 in this MEP document (https://www.gov.cn/xinwen/2016–11/23/content_5136542.htm, accessed on 20 Dec 2022) is about disguised pollution at night in Inner Mongolia. Case 12 is about disguised pollution at night in Jiangsu Province.

[19] One possible explanation is that the local government does not take action before the central inspection team's arrival and only starts to impose stricter regulations and supervision on firms upon the arrival of the inspectors in the city. Therefore, the largest reduction effect on disguised pollution should occur in the last week of the inspection period, with the gradual entry of central inspectors to different cities of the province and more and more cities in the province taking action. In our sample, 90% of the inspections last for four weeks, which makes it reasonable to expect the largest effect in the fourth week.

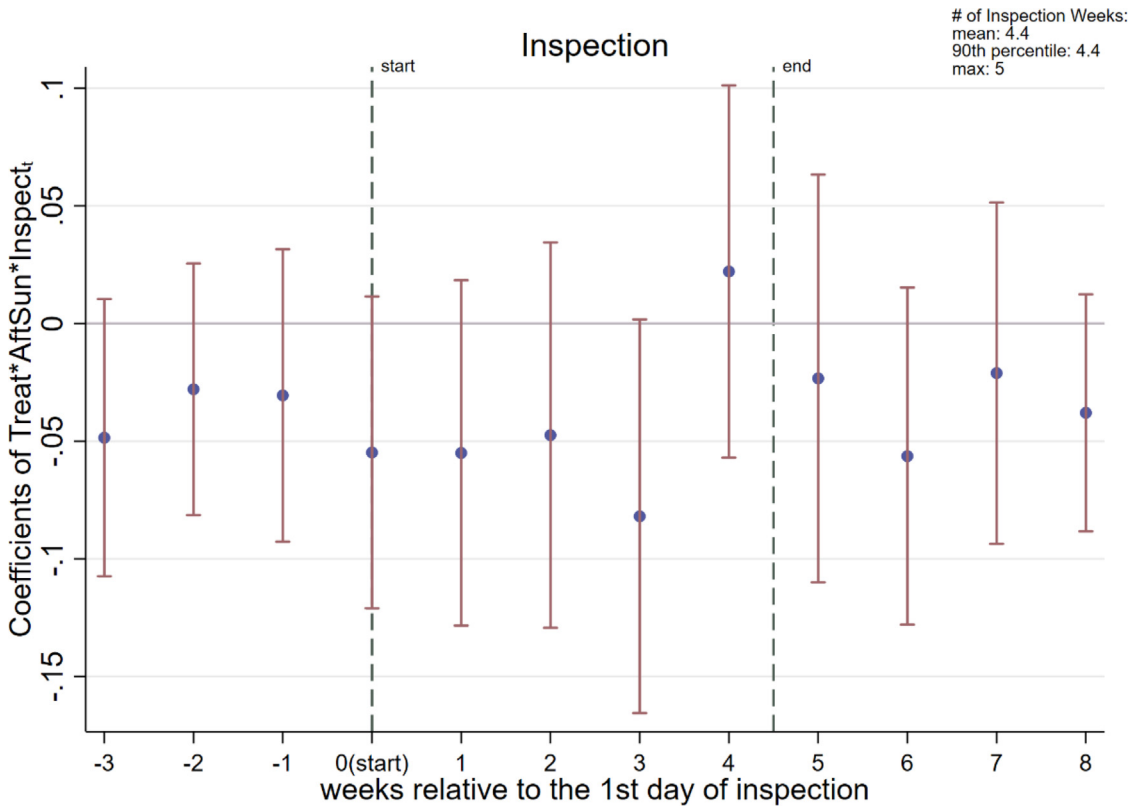

Fig. 5. Inspection. This figure presents the coefficients and 95% confidence intervals of $Treat \times Sunset \times Inspect_t$, namely the dynamic effects of inspection on disguised pollution at the weekly level. The benchmark is the period from the beginning of the data to three weeks before the inspection. Week 0 denotes the week when the inspection starts.

tions only reduce sulfur dioxide emissions over a five-week period. Additionally, from a long-term perspective, columns 1 and 2 of Appendix Table A5 show that the inspection, on average, does not correlate with a statistically significant reduction of disguised pollution, although the coefficients are negative. In summary, our results suggest that inspection by MEP officials may have a limited and temporary impact in reducing disguised pollution in the short-term; however, inspection alone may not be an effective long-term solution for reducing disguised pollution.Table A6.

6.1.3. Economic growth pressure

In general, there is a tradeoff between pollution abatement and local economic growth for local governors. More strict enforcement of environmental regulations may hurt the GDP growth rate of the local region. In this subsection, we aim to understand whether disguised pollution is more severe when the local government faces more downward pressure on economic growth. In saying that, we interact the GDP growth rate of a city in the previous year with the DD term ($Sunset_{it} \times T_i$), controlling for all the pairwise and main terms. As presented in Table 9, the DDD coefficient is significantly negative in columns 1 and 2, suggesting that a 1% lower GDP growth rate in the previous year increases the magnitude of the disguised pollution effect by 11.1–12.7% (0.007/0.063 = 11.1% ; 0.008/0.063 = 12.7%). The DDD coefficient in column 3 is not statistically significant, which is likely due to the smaller sample size.

The finding above may also explain a puzzle: local governments should also have access to environmental monitoring data. Why can't the governors identify the areas affected by disguised pollution from the data and search for the firms engaging in such behavior? The tradeoff between GDP growth rate and disguised pollution may suggest collusion between local governors and industrial firms: local governors are more likely to tolerate disguised pollution if the GDP growth rate is unpromising.

Table 9
GDP growth and disguised pollution.

VARIABLES	(1) lnso2	(2) lnso2	(3) lnso2
	full-192 cities	40vs20 + restrict-71 cities	restricted-33 cities
Treat*AftSun	0.125***	0.110***	0.089**
	(0.040)	(0.023)	(0.036)
Treat*AftSun*GDP GrowthRate in previous year	−0.008**	−0.007***	−0.005
	(0.004)	(0.002)	(0.004)
Observations	3,608,649	2,762,405	1,144,133
R-squared	0.490	0.533	0.503
Atmospheric conditions	Yes	Yes	Yes
Date FE	Yes	Yes	Yes
Station-Year FE	Yes	Yes	Yes
City-Hour FE	Yes	Yes	Yes
Cluster	city date	city date	city date

NOTES: This table reports the heterogeneity analysis by interacting the DID term with the GDP growth rate of the previous year for the matched cities. All pairwise interactions and main effects are controlled for. In Column 1, we use the regression sample of our main analysis, which includes the top 20% and bottom 20% of stations in terms of the number of factories in SO_2-intensive industries. In Column 2, we restrict the sample to 71 cities that host at least one treatment and one control station, but under the criteria of top 40% or bottom 20% in terms of the number of factories in SO_2 intensive industries. In Column 3, we further restrict the sample to 33 cities that have at least one treatment (top 20%) and one control (bottom 20%) station. Standard errors are robustly two-way clustered at city and date levels. *P < 0.10;**P < 0.05;***P < 0.01.

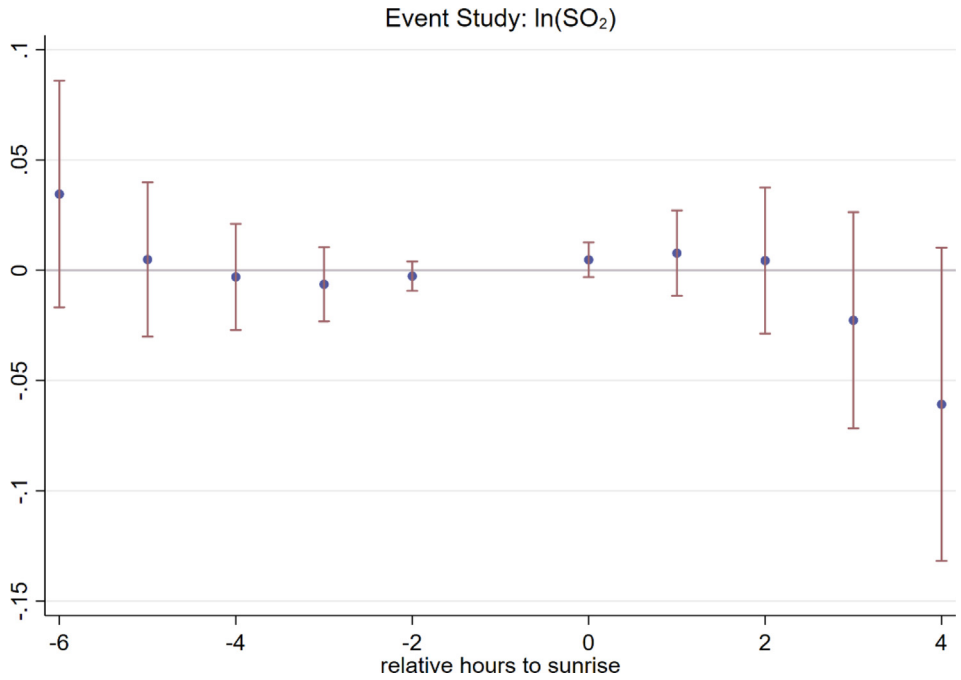

Fig. 6. Event study (sunrise). This figure presents the coefficients and 95% confidence interval of the event study of sunrise. The event time is the sunrise hour. The sample is six hours before sunrise, the sunrise hour, and four hours after sunrise. The baseline average is the first hour before sunrise. The coefficient estimates are available in Table A3.

6.2. The effect of sunrise

In this subsection, we investigate the effect of sunrise on pollution concentration. Our hypothesis is that firms stop the processes and behaviors associated with disguised emission prior to sunrise or at sunrise and then conduct normal compliant production with scrubbers turned on, hence the pollution gap between the treatment group and control group should narrow after sunrise.

Let us consider two scenarios. In the first scenario, all polluting firms stop their disguised discharge behavior *at* sunrise. We would then expect to observe a trend opposite to that seen in the event study for sunset, whereby the difference between the treatment and control groups would be positive before sunrise due to the presence of disguised pollution behavior, and then gradually decrease and converge after sunrise as pollutants disperse. In the second scenario, all polluting firms stop their illicit discharge behavior several hours *before* sunrise. In this case, we would expect the difference between the two groups to begin decreasing and converging before sunrise. To test these hypotheses, we conduct an event study using the regression specification of Eq. (4); the estimated coefficients of the dynamic effects are plotted in Fig. 6.

Fig. 6 shows that the gap between the two groups decreases before and after sunrise, which indicates a hybrid of these two scenarios. In reality, firms of different types or sizes may cease their illicit discharge at different times due to production cost considerations. That is, some firms may only discharge for a few hours at night, while others may continue to discharge throughout the night until sunrise. In this case, we would observe the trend shown in Fig. 6: compared to the first hour before sunrise, the gap between the two groups gradually decreases from positive (insignificant) to zero before sunrise, indicating a downward pretrend caused by firms that ceased discharging a few hours before sunrise. The continued decrease in the gap between the two groups three hours after sunrise is likely due to the last group of polluting firms, which ceased discharging at sunrise. However, we recognize that due to the lack of firm-level information, we cannot test this heterogeneity at the station level.

We acknowledge that the event study for sunrise faces several challenges in the research design. First, due to the presence of disguised emissions, the treatment and control groups are naturally incomparable at night (prior to sunrise), making it difficult to obtain an unbiased estimate in the event study and interpret the post-sunrise coefficients. Therefore, all that we try to show is the trend of pollution change between the treatment and control groups pre- and post-sunrise, as presented in Fig. 6. Second, although the gap between the two groups is estimated to decrease after sunrise, we still need to be cautious about the estimated values of the post-sunrise coefficients. The post-sunrise estimates tend to be biased due to the presence of the pre-trends before sunrise (Roth, 2022). In Fig. A8, the blue dashed line represents the expected value of the coefficients conditional on passing the pretest under the hypothesized trend—47% of the magnitude of the coefficient in the fourth hour after sunrise is composed of the bias brought by the pre-trend. It is important to carefully consider these biases when interpreting the coefficients.

To summarize, as shown in Fig. 6, we find an overall downward-sloping trend around sunrise, although the post-sunrise coefficients should be interpreted with caution. This downward pattern indicates the gap between the two groups gradually narrows around sunrise due to the cessation of disguised emissions by polluting firms.

6.3. Firm-level analysis

In this subsection, we employ firm-level data to understand the sources of disguised pollution. To monitor the emission activities of major polluters, the MEP installed monitors in big firms in the polluting sectors to monitor their hourly emissions. Such data is available on platforms accessible to the public. In this section, we aim to understand whether the increase in pollution after sunset is from the emissions of the monitored firms. Specifically, we compare the hourly emission levels of SO_2 and the compliance rate before and after sunset in 135 firms in three cities in Hebei province and 177 firms in all the cities in Zhejiang province covered

Table 10
Effect of sunset on monitored firms.

	(1)	(2)	(3)	(4)	(5)	(6)	(7)	(8)
	lnso2				compliance			
Sunset	0.009	0.002	0.016	0.014	−0.001	−0.0003	−0.006**	−0.006**
	(0.013)	(0.010)	(0.029)	(0.028)	(0.001)	(0.001)	(0.003)	(0.003)
Sunset*KeyRegion			−0.008	−0.013			0.006**	0.006**
			(0.030)	(0.030)			(0.003)	(0.003)
Observations	1,153,076	1,064,361	1,153,076	1,064,361	1,272,046	1,174,577	1,272,046	1,174,577
Benchmark average	/				0.951	0.951	0.951	0.951
R-squared	0.493	0.493	0.493	0.493	0.621	0.620	0.621	0.620
Atmospheric conditions		Yes		Yes		Yes		Yes
Firm-Chimney-Year FE	Yes	Yes	Yes	Yes	Yes	Yes	Yes	Yes
Date FE	Yes	Yes	Yes	Yes	Yes	Yes	Yes	Yes
Hour FE	Yes	Yes	Yes	Yes	Yes	Yes	Yes	Yes
Cluster	firm date	firm date	firm date	firm date	firm date	firm date	firm date	firm date

NOTES: This table uses hourly monitored data in 135 firms in Hebei and 177 firms in Zhejiang. Compliance is a dummy variable equal to one if the hourly observation measured by CEMS is non-missing and below the emission standard, otherwise zero. KeyRegion is a dummy equal to one if the firm is in the key region (47 prefectures) that are strictly monitored by Ministry of Environmental Protection, otherwise zero. All regressions control for firm-chimney-year, date, and hour fixed effects. The time period is 2015. Standard errors are robustly two-way clustered at firm and day level. *P < 0.10;**P < 0.05;***P < 0.01.

by CEMS. For each firm, we can know the hourly emission level of the three main pollutants, as well as whether the hourly emissions exceed the threshold set by the MEP. Karplus et al. (2018) discuss the possibility that CEMS data may be manipulated downward in the 47 cities within the key regions for pollution alleviation.[20] Therefore we also interact the Sunset dummy with a dummy variable indicating the key regions.

Table 10 presents the estimation results. From columns 1 to 4, we do not find monitored firms increase their emissions after sunset, which suggests that the automation in pollution monitoring at the firm level is effective in regulating the phenomenon of disguised pollution. However, Karplus et al. (2018) document that plant managers have incentives to falsify or selectively omit concentration data when facing stricter new standards and greater pressure to comply. According to the requirement of CEMS, emissions should be reported every hour of the day at each monitoring unit (chimney). Following Karplus et al. (2018), we define a new variable—firm compliance—a dummy variable equal to one if the hourly observation measured by CEMS is available and below the emission standard, otherwise zero. As shown in columns 5 and 6, we find that firm compliance falls slightly after sunset (insignificant), and firms in key regions are significantly more compliant than firms in non-key regions (columns 7 and 8), which echoes Karplus et al. (2018)'s finding of behavior disparities between the key region and non-key region. The magnitude of such difference is relatively small though (approximately 0.5% drop from the benchmark compliance rate).

Our findings show that CEMS, as an automated real-time pollution monitoring system, is effective in reducing disguised pollution, which is consistent with Greenstone et al. (2022)'s finding that automation in air pollution monitoring improves the data quality and thus contributes to pollution regulation. Our findings that the difference in the firm compliance rate before and after sunset varies depending on the intensity of regulation also suggests that CEMS is not a panacea, and needs to be coordinated with local regulatory instruments in order to have the greatest effect.

7. Conclusion

In conclusion, by comparing the hourly readings in air pollution monitoring stations surrounded by high factory density with stations surrounded by low factory density, we find that the industrial toxin SO_2 significantly increases after sunset in the treated stations. This effect is robust to different definitions of treatment and control stations. In exploiting the high-frequency emission data of firms monitored by CEMS, we do not find such a pattern. Therefore, our result is likely driven by the unmonitored small firms that can disguise their polluting behaviors under cover of the night.

Our findings provide a better understanding of industrial firms' polluting behavior. The monitoring stations are not randomly located but target heavily polluted industrial areas in cities. Despite this fact, firms near the stations still engage in disguised pollution at night because they are not directly monitored by the MEP. They rely on the large population of polluting firms around these monitoring stations to mask their polluting behavior, especially at night. In contrast, monitored large firms do not engage in disguised pollution at night, and inspections by site visit only temporarily mitigate such behavior when MEP officials are present. Therefore, our results call for a more comprehensive environmental monitoring system in China that not only covers large firms in the key sectors, but also the small firms in SO_2-intensive industries. Improving the coverage and technology of monitoring systems would be helpful in detecting regulatory noncompliance which is prevalent not only in China but also in other developing countries (Duflo et al., 2013; Greenstone et al., 2022).

Our findings in this paper establish the link between firms' industrial activities and air pollution. Environmental regulation is crucial for emission reduction in the industrial sector (Shapiro and Walker, 2018). Furthermore, in China's context, disguised pollution by unmonitored industrial firms may generate significant welfare losses to society. Existing literature already documents the causal link between air pollution and health consequences, both physically and mentally (Chen et al., 2013; Ebenstein et al., 2017; Zhang et al., 2018a; 2018b; Zheng et al., 2019). Following the calculation in Barwick et al. (2018) that a 10 $\mu g/m^3$ reduction in $PM_{2.5}$ would lead to 144.5 and 59.6 billion yuan of mortality and morbidity savings, respectively, we can carry out a back-of-the-envelope calculation to quantify the benefit in terms of health savings if disguised pollution is stopped. The costs of stopping disguised pollution, as indicated in our analysis, would largely be in the installation of CEMS in all SO_2 emitters (instead of only large emitters as is currently the case). As shown in Appendix Table A7, the fixed cost and operating cost of CEMS (22 billion yuan per year) can be justified by the improved health benefits following pollution reduction (29.2 billion yuan per year). It is also worth

[20] Please see Table A.6 in the Appendix for a list of these 47 cities.

noting that the health benefits may only represent a lower bound of the total benefits of improved air quality, without factoring in the benefits of productivity improvements and the reduction of behavioral mistakes, among others. Therefore, we recommend the adoption of CEMS by the whole sector of industrial polluters, as this is likely to effectively improve air quality through a reduction in disguised pollution.

Disclosure statement

There is no conflict of interest to be disclosed related to the submitted paper, titled "Disguised Pollution: Industrial Activities in the Dark".

Data availability

Data will be made available on request.

Declaration of Competing Interest

The authors declare that they have no known competing financial interests or personal relationships that could have appeared to influence the work reported in this paper.

Appendix A

Figs. A1–A8 and Tables A1–A7

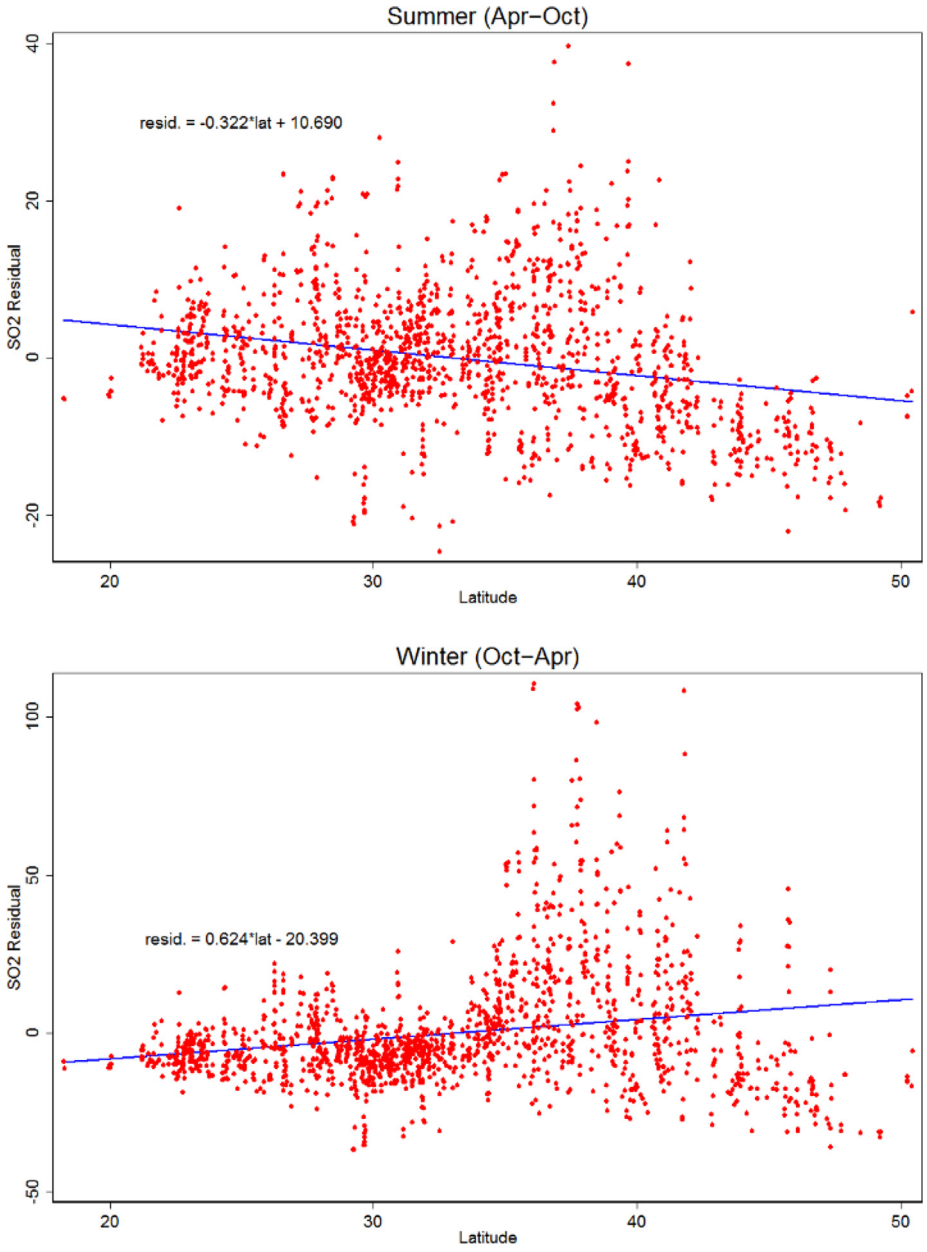

Fig. A1. SO_2 and latitude in summer and winter. In this figure, we plot the residual of SO_2 after taking out date and hour fixed effects and weather controls, against the latitude of each monitoring station in summer time (when higher latitude is associated with longer daytime) and winter time (when higher latitude is associated with shorter daytime). A linear fit of the scatter plot is also presented in the figure.

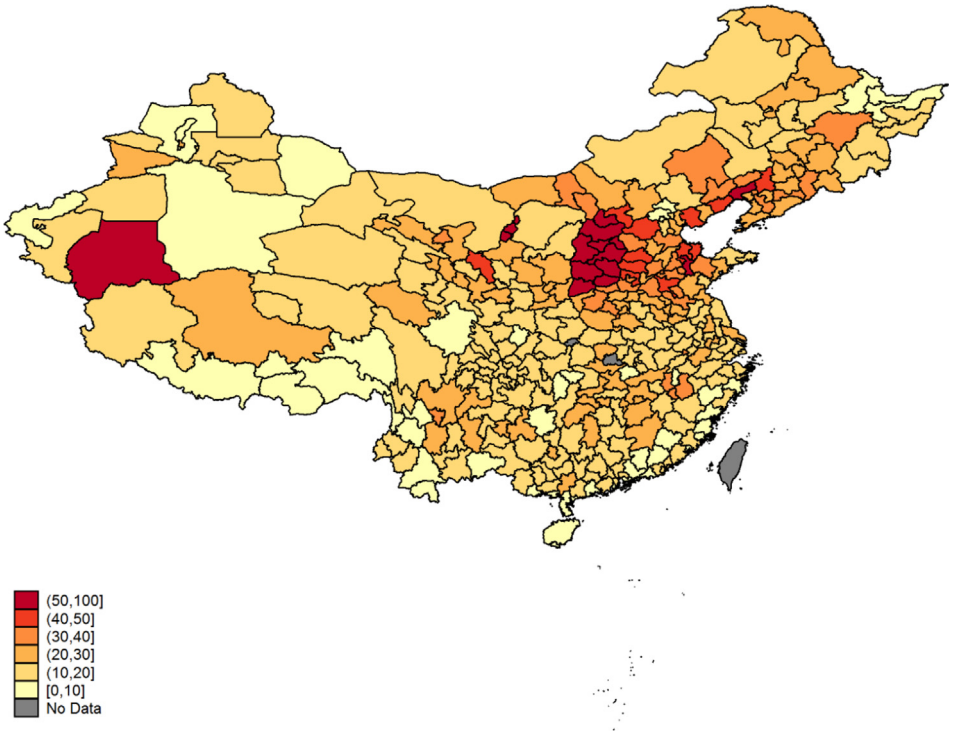

Fig. A2. Average hourly SO_2 in 1,583 monitoring stations, 2015–2017. We plot the average hourly SO_2 in 1,583 monitoring stations from 2015 to 2017 on this map. The Ministry of Environmental Protection (MEP) publishes hourly measures of $PM_{2.5}$, PM_{10}, CO, SO_2, NO_2, O_3, and AQI for each station every hour. Our data is downloaded from https://beijingair.sinaapp.com/, the data source of which is the National Urban Air Quality Live Update Platform (https://106.37.208.233:20035/).

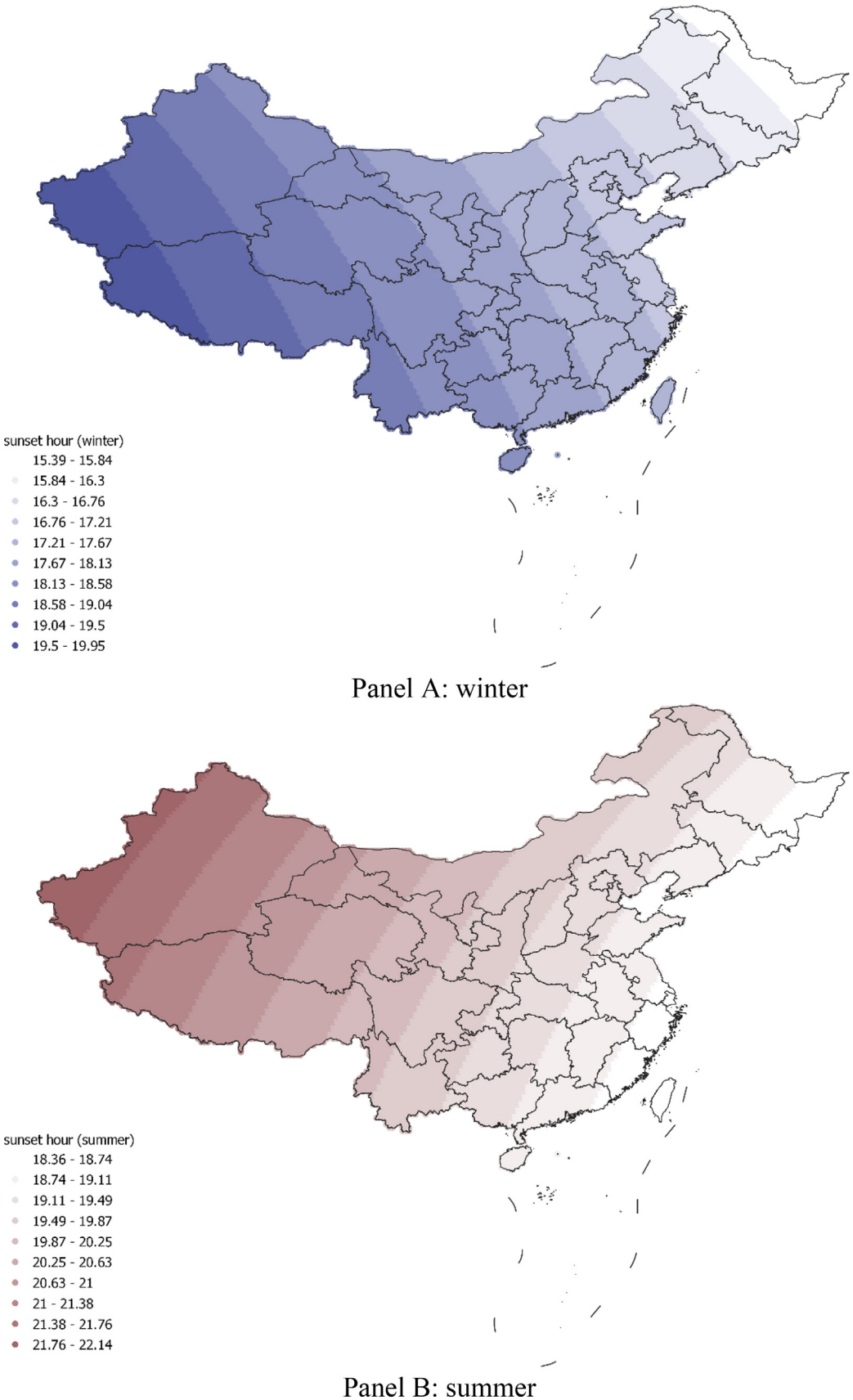

Fig. A3. Sunset hours in winter and summer, by longitude bins. Panel A presents the sunset hour in winter by different longitude bins, and Panel B presents the summer sunset hour by different longitude bins.

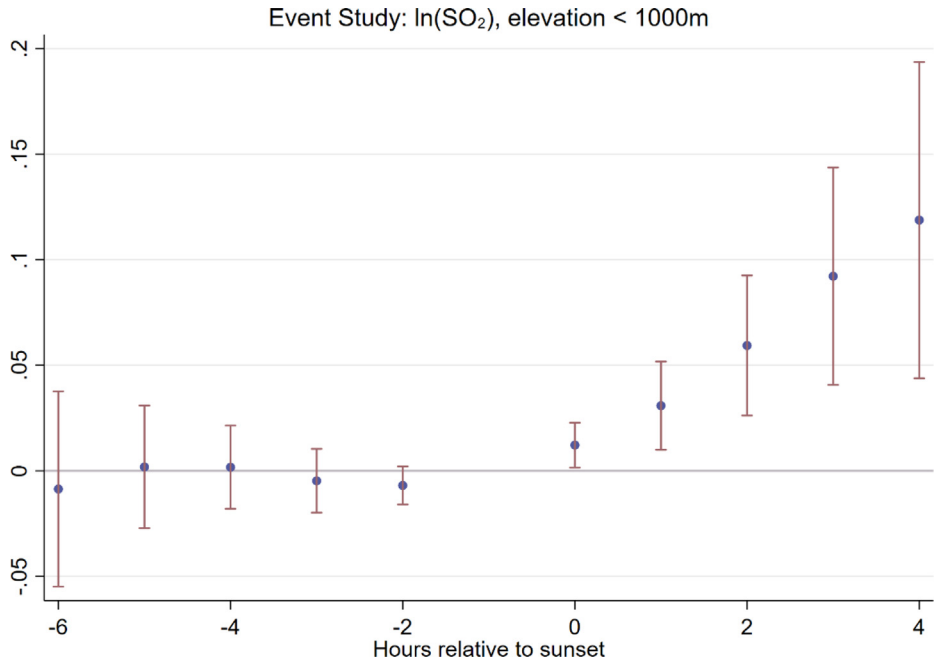

Fig. A4. Event study for the sample with elevation less than 1,000 m. This figure presents the coefficients and 95% confidence interval of the event study for the low-elevation sample. The event time is the sunset hour. The baseline average is the first hour before sunset.

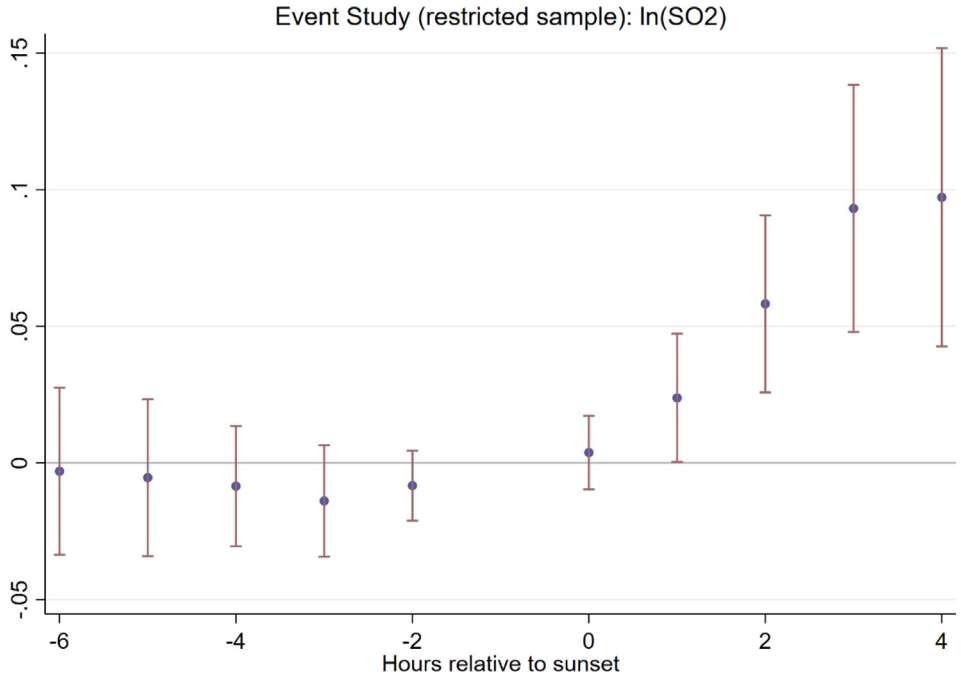

Fig. A5. Event study of the restricted sample. This figure presents the coefficients and 95% confidence interval of the same event study as Fig. 3, except that the sample is the restricted sample. The event time is the sunset hour. The baseline average is the first hour before sunset.

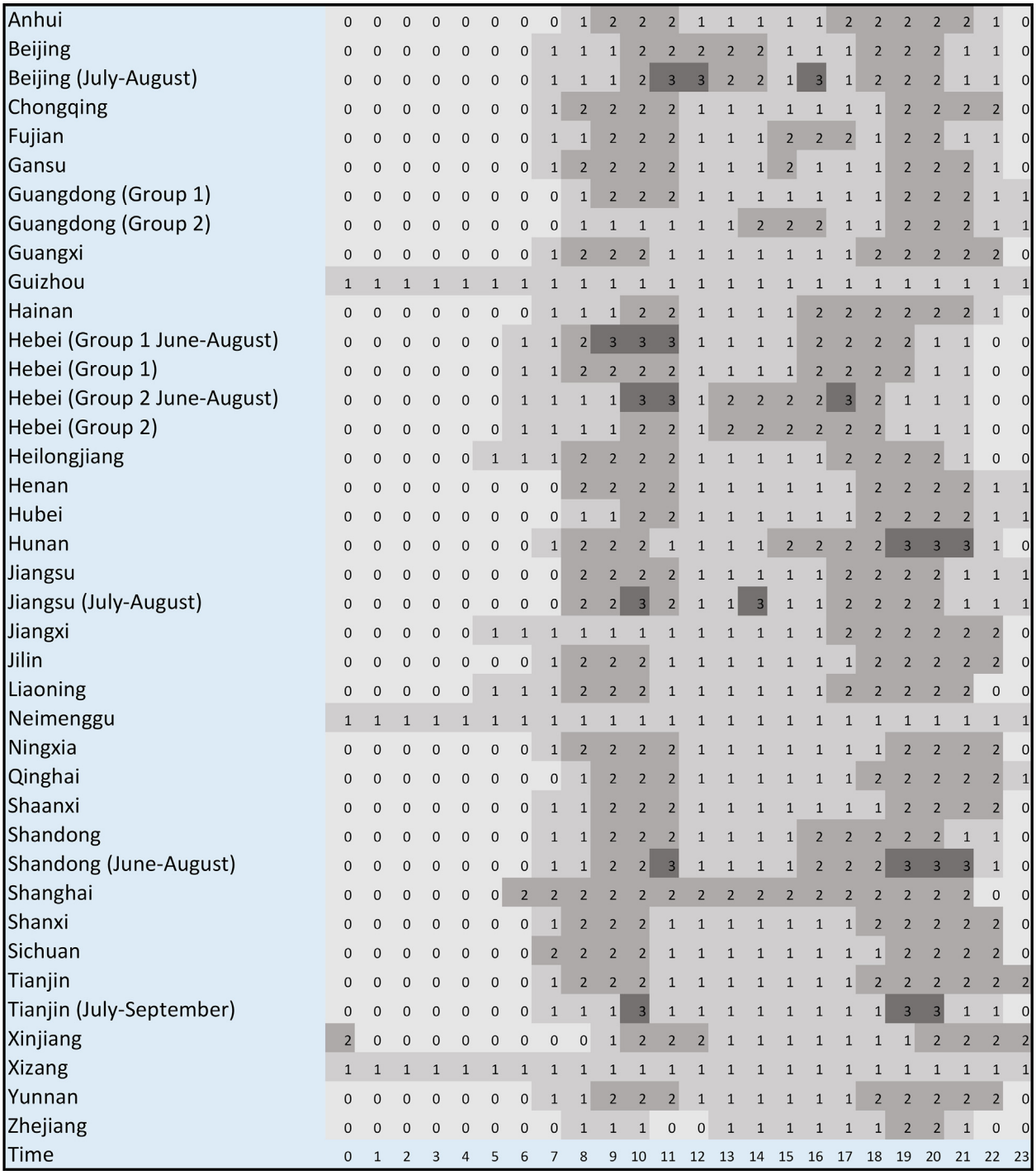

Fig. A6. Electricity price within a day. The figure presents electricity price variations within a day in different provinces in China. Each row represents a province, and each column represents an hour. "0" represents off-peak (level 1); "1" represents off-peak (level 2); "2" represents peak (level 1), and "3" represents peak (level 2). Therefore, the larger the number, the higher the electricity price. The information is collected manually by the authors from various sources.

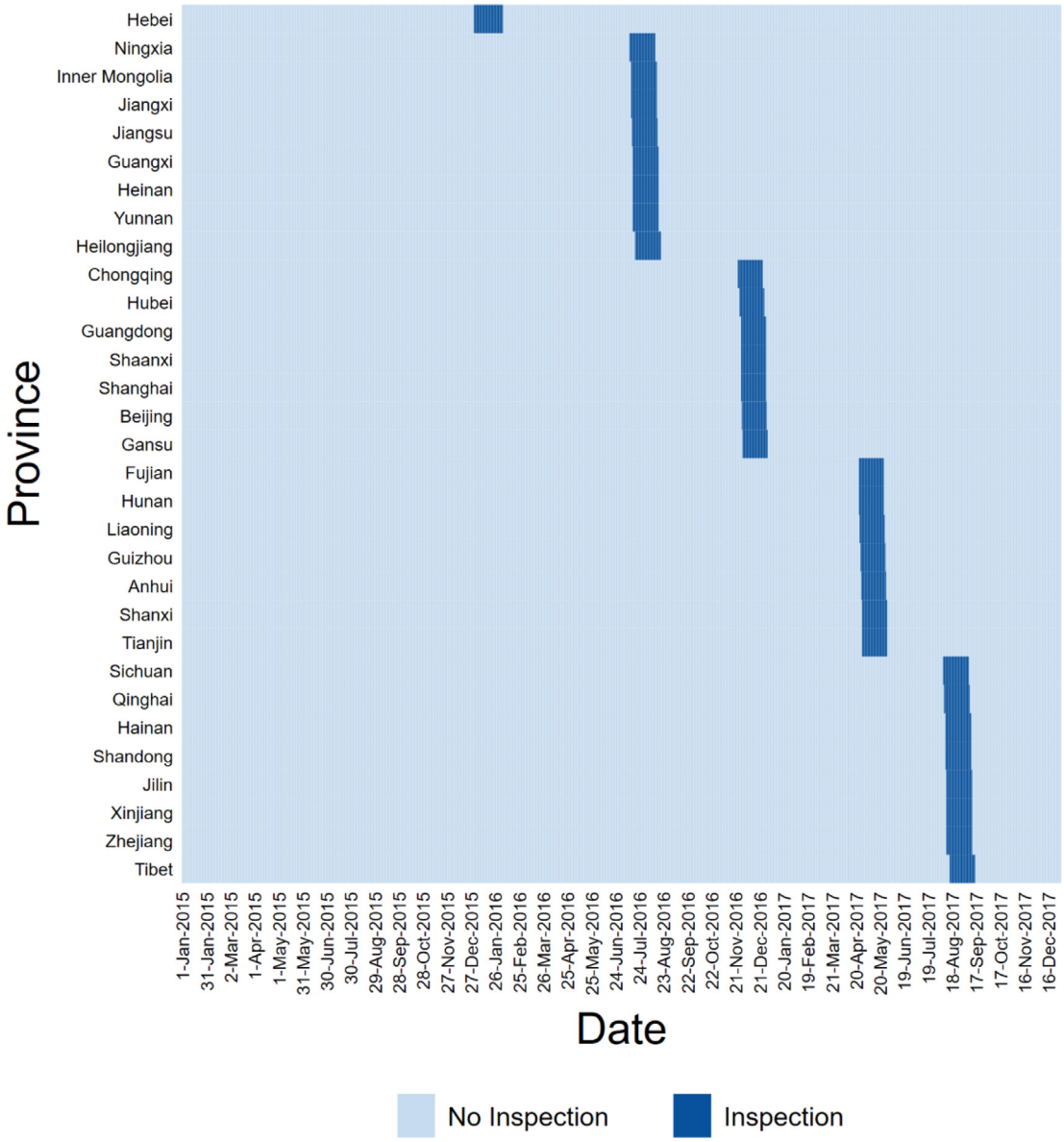

Fig. A7. Timeline for the central inspections of different provinces. This figure plots the timeline for the central inspection from 2015 to 2017.

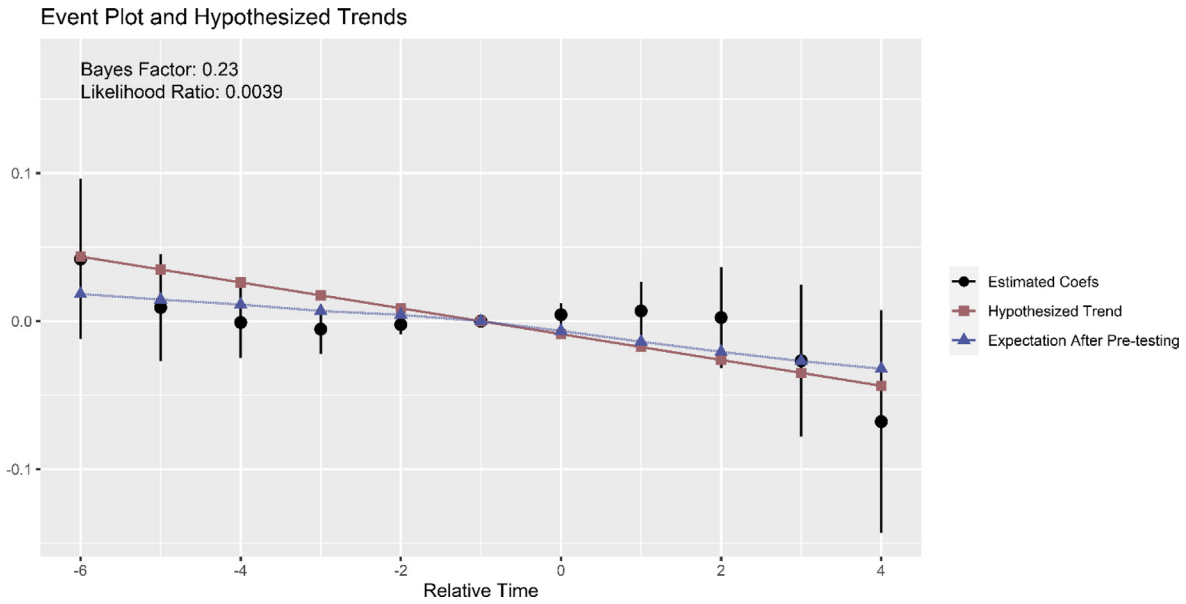

Fig. A8. Pre-trends test for sunrise. This figure presents the pre-trends test proposed by Roth (2022). The analysis suggests that we can detect a negative linear trend of a magnitude of −0.0087 (the slope of the red line) or greater (in absolute terms) with 80% power in our event study. The mean after pre-testing at hour 4 is −0.032, accounting for about 47% of the estimate.

Table A1
Robustness - exclude all diesel truck allowed hours.

VARIABLES	(1) lnso2	(2) lnso2
Treat*Sunset	0.064***	0.070***
	(0.023)	(0.022)
Observations	2,414,220	2,805,567
R-squared	0.507	0.500
sample	exclude-city-day	exclude-all-hours
Atmospheric conditions	Yes	Yes
Date FE	Yes	Yes
Station-Year FE	Yes	Yes
City-Hour FE	Yes	Yes
Cluster	city date	city date

NOTES: This table reports the regression results using data that excludes the "post sunset, truck allowed" observations. There are 138 cities with detailed timing of diesel truck restrictions which consists of our regression sample. The time period is from 2015 to 2017. Standard errors are robustly two-way clustered at city and date levels. *P < 0.10;**P < 0.05;***P < 0.01.

Table A2
Robustness – using different radius to define treatment.

VARIABLES	(1) lnso2	(2) lnso2
Treat*Sunset	0.078***	0.073***
	(0.023)	(0.027)
Observations	3,561,552	3,366,118
R-squared	0.493	0.498
Radius	4 km	5 km
Atmospheric conditions	poly	poly
Station-Year FE	Yes	Yes
Date FE	Yes	Yes
City-Hour FE	Yes	Yes
Cluster	city date	city date

NOTES: This table alters the radius from 3 km to 4 km and 5 km when defining the treatment and control stations. All columns use 429 monitoring stations in 192 cities. The time period is from 2015 to 2017. Standard errors are robustly two-way clustered at city and date levels. *P < 0.10;**P < 0.05;***P < 0.01.

Table A3
Regression table for event study in Fig. 3 (sunset) and Fig. 6 (sunrise).

VARIABLES	(1) lnso2 (sunset)	(2) lnso2 (sunrise)
Treat*6 h before	−0.030	0.035
	(0.025)	(0.026)
Treat*5 h before	−0.017	0.005
	(0.016)	(0.018)
Treat*4 h before	−0.013	−0.003
	(0.011)	(0.012)
Treat*3 h before	−0.017**	−0.006
	(0.008)	(0.009)
Treat*2 h before	−0.015***	−0.003
	(0.005)	(0.003)
Treat*sunset or sunrise	0.018***	0.005
	(0.006)	(0.004)
Treat*1 h after	0.036***	0.008
	(0.010)	(0.010)
Treat*2 h after	0.056***	0.004
	(0.016)	(0.017)
Treat*3 h after	0.081***	−0.023
	(0.026)	(0.025)
Treat*4 h after	0.108***	−0.061*
	(0.038)	(0.036)
Observations	4,099,314	4,063,793
R-squared	0.489	0.508
Atmospheric conditions	Yes	Yes
Date FE	Yes	Yes
Station-Year FE	Yes	Yes
City-Hour FE	Yes	Yes
Cluster	city date	city date

NOTES: This table presents the regression results for the event study with respect to sunset and sunrise respectively. The regression model is specified in Eq. (2). The time period is from 2015 to 2017. Standard errors are robustly two-way clustered at city and date levels. *P < 0.10;**P < 0.05;***P < 0.01.

Table A4
Effect of sunset on monitored firms' production.

VARIABLES	(1) ln(flue gas flow)	(2)	(3) ln(flue gas flow rate)	(4)
Sunset	−0.0005	0.017	0.008	0.026
	(0.013)	(0.028)	(0.010)	(0.019)
Observations	46,144	42,463	51,646	47,516
R-squared	0.711	0.709	0.454	0.454
Benchmark	11.894	11.898	1.539	1.538
Atmospheric conditions		Yes		Yes
Firm-Chimney-Year FE	Yes	Yes	Yes	Yes
Date FE	Yes	Yes	Yes	Yes
Hour FE	Yes	Yes	Yes	Yes
Cluster	firm date	firm date	firm date	firm date

NOTES: This table uses hourly monitored data of 34 firms in Zhejiang that reports flue gas flow or flue gas flow rate. Flue gas flow and flue gas flow rates are proxies for production. All regressions control for firm-chimney-year, date, and hour fixed effects. The time period is 2015. Standard errors are robustly two-way clustered at firm and day level. *P < 0.10;**P < 0.05;***P < 0.01.

Table A5
Impact of MEP inspection on disguised pollution.

VARIABLES	(1) lnso2	(2) lnso2	(3) lnso2
Treat*Sunset	0.063***	0.066***	0.077***
	(0.018)	(0.020)	(0.028)
Treat*Sunset*Inspect	−0.013	−0.016	
	(0.020)	(0.021)	
Treat*Sunset*After Inspection		−0.012	
		(0.012)	
Treat*Sunset*3 weeks before inspection			−0.049
			(0.030)
Treat*Sunset*2 weeks before inspection			−0.028
			(0.027)
Treat*Sunset*1 week before inspection			−0.031
			(0.032)
Treat*Sunset*1st week of inspection			−0.055
			(0.034)
Treat*Sunset*2nd week of inspection			−0.055
			(0.037)
Treat*Sunset*3rd week of inspection			−0.047
			(0.042)
Treat*Sunset*4th week of inspection			−0.082*
			(0.042)
Treat*Sunset*5th week of inspection			0.022
			(0.040)
Treat*Sunset*1 week after inspection			−0.023
			(0.044)
Treat*Sunset*2 weeks after inspection			−0.056
			(0.036)
Treat*Sunset*3 weeks after inspection			−0.021
			(0.037)
Treat*Sunset*4 weeks after inspection			−0.038
			(0.026)
Observations	4,099,314	4,099,314	1,534,298
R-squared	0.487	0.487	0.489
Atmospheric conditions	Yes	Yes	Yes
Date FE	Yes	Yes	Yes
Station-Year FE	Yes	Yes	Yes
City-Hour FE	Yes	Yes	Yes
Cluster	city date	city date	city date

NOTES: This table presents the analysis of the impact of central inspection. Columns 1 and 2 report the average effect of inspection on disguised pollution. Column 3 shows the dynamic effects (plotted in Fig. 5). We also control for all the pairwise interactions and main effects in the regressions. The time period is from 2015 to 2017. Standard errors are robustly two-way clustered at city and date levels. *P < 0.10;**P < 0.05;***P < 0.01.

Table A6
List of cities in the key regions.

Yangtze River Delta Region							
Shanghai	Nanjing	Wuxi	Changzhou	Suzhou	Nantong	Yangzhou	Zhenjiang
Taizhou	Hangzhou	Ningbo	Jiaxing	Huzhou	Shaoxing		
Pearl River Delta Region							
Zhuhai	Foshan	Dongguan	Zhongshan	Jiangmen	Huizhou	Zhaoqing	Guangzhou
Shenzhen							
Beijing-Tianjin-Hebei Region							
Beijing	Tianjin	Shijiazhuang	Tangshan	Baoding	Langfang		
Others							
Jinan	Qingdao	Zibo	Weifang	Rizhao	Wuhan	Changsha	Chongqing
Chengdu	Fuzhou	Sanming	Taiyuan	Xi'an	Xianyang	Lanzhou	Yinchuan
Urumqi	Shenyang						

NOTES: We define key regions as the 47 prefectures that are closely monitored by the Ministry of Environmental Protection in terms of pollution. These 47 prefectures account for 14% of total land area, 48% of the total population, 71% of the economic size in China, and consume 52% of coal, produce 48% of SO_2, 51% NO_x, 42% particulate matter, and approximately 50% VOC (Rohde and Muller, 2015).

Table A7
Cost-benefit Analysis.

Cost (billion yuan value per year)	Value
CEMS fixed cost	6
CEMS operating cost	16
Total cost	22
Health savings	
Morbidity	8.5
Mortality	20.7
Total health savings	29.2

NOTES: The fixed cost and operating cost of full adoption of CEMS systems in China are obtained from the 2018 Environmental Monitoring Market Forecast (https://www.zghbcy.com/templ/news_xxym.html?articleId = 1330&categoryId = 16). The estimated mortality and morbidity savings of lower $PM_{2.5}$ concentration level are from Barwick et al. (2018), who find that 10 $\mu g/m^3$ reduction in $PM_{2.5}$ would lead to 144.5 and 59.6 billion *yuan* of mortality and morbidity savings, respectively. In the back-of-the-envelope calculation, we adjust the value of health savings according to the average treatment effect of disguised pollution on $PM_{2.5}$ concentration 2.6%) together with the average $PM_{2.5}$ levels (around 55 $\mu g/m^3$ in 2017) in China. Therefore, the estimated morbidity cost is (0.026*55)/10*59.6 = 8.5 billion yuan, and the estimated mortality cost is (0.026*55)/10*144.5 = 20.7 billion yuan.

References

Agarwal, S., Qian, W., Seru, A., Zhang, J., 2020. Disguised corruption: Evidence from consumer credit in China. J. Financ. Econ. 137, 430–450.

Alexander, D., Schwandt, H., 2022. The Impact of Car Pollution on Infant and Child Health: Evidence from Emissions Cheating. The Review of Economic Studies.

Barwick, P.J., Li, S., Rao, D., Zahur, N.B., 2018. The Healthcare Cost of Air Pollution: Evidence from the World's Largest Payment Network. NBER working paper 24688.

Chen, Y., Ebenstein, A., Greenstone, M., Li, H., 2013. Evidence on the impact of sustained exposure to air pollution on life expectancy from China's Huai River policy. Proc. Natl. Acad. Sci. 110, 12936–12941.

Chen, Y.J., Li, P., Lu, Y., 2018. Career concerns and multitasking local bureaucrats: Evidence of a target-based performance evaluation system in China. J. Dev. Econ. 133, 84–101.

Corripio, J.G., 2003. Vectorial algebra algorithms for calculating terrain parameters from DEMs and solar radiation modelling in mountainous terrain. Int. J. Geogr. Inf. Sci. 17, 1–23.

Deng, Y., Wei, S., Wu, J., 2015. Estimating the unofficial income of officials from housing purchases: The case of China. National University of Singapore Working paper.

Duflo, E., Greenstone, M., Pande, R., Ryan, N., 2013. Truth-telling by third-party auditors and the response of polluting firms: Experimental evidence from India. The Quarterly Journal of Economics 128, 1499–1545.

Duflo, E., Greenstone, M., Pande, R., Ryan, N., 2018. The value of regulatory discretion: Estimates from environmental inspections in India. Econometrica 86, 2123–2160.

Ebenstein, A., Fan, M., Greenstone, M., He, G., Zhou, M., 2017. New evidence on the impact of sustained exposure to air pollution on life expectancy from China's Huai River Policy. Proc. Natl. Acad. Sci. 114, 10384–10389.

Eckert, H., 2004. Inspections, warnings, and compliance: the case of petroleum storage regulation. J. Environ. Econ. Manag. 47, 232–259.

Finer, D.A., 2018. What insights do taxi rides offer into Federal Reserve leakage? Chicago Booth: George J. Stigler Center for the Study of the Economy & the State Working Paper.

Grainger, C., Schreiber, A., Chang, W., 2018. Do regulators strategically avoid pollution hotspots when siting monitors? Evidence from remote sensing of air pollution. University of Wisconsin unpublished manuscript.

Greenstone, M., He, G., Jia, R., Liu, T., 2022. Can Technology Solve the Principal-Agent Problem? Evidence from China's War on Air Pollution. American Economic Review: Insights 4, 54–70.

Halliday, E., Kemeny, E., 1964. The effect of Sunrise and Sunset on the Concentration of Atmospheric Pollutants. Int. J. Air Wat. Pollut. 8, 43–47.

Hanna, R.N., Oliva, P., 2010. The impact of inspections on plant-level air emissions. BE J. Econ. Anal. Policy 10.

He, G., Wang, S., Zhang, B., 2020. Watering down environmental regulation in China. Quart. J. Econ. 135, 2135–2185.

Henriques, I., Sadorsky, P., 1996. The determinants of an environmentally responsive firm: An empirical approach. J. Environ. Econ. Manag. 30, 381–395.

Karatepe, N., 2000. A comparison of flue gas desulfurization processes. Energy Source. 22, 197–206.

Karplus, V.J., Wu, M., 2019. Smoke and Mirrors: Did China's Environmental Crackdowns Lead to Persistent Changes in Polluting Firm Behavior? Working paper.

Karplus, V.J., Zhang, S., Almond, D., 2018. Quantifying coal power plant responses to tighter SO2 emissions standards in China. Proc. Natl. Acad. Sci. 115, 7004–7009.

Keohane, N.O., Mansur, E.T., Voynov, A., 2009. Averting regulatory enforcement: Evidence from new source review. J. Econ. Manag. Strateg. 18, 75–104.

Kuerban, M., Waili, Y., Fan, F., Liu, Y., Qin, W., Dore, A.J., Peng, J., Xu, W., Zhang, F., 2020. Spatio-temporal patterns of air pollution in China from 2015 to 2018 and implications for health risks. Environ. Pollut. 258, 113659.

Mu, Y., Rubin, E.A., Zou, E., 2021. What's Missing in Environmental (Self-) Monitoring: Evidence from Strategic Shutdowns of Pollution Monitors. National Bureau of Economic Research.

Raynor, G.S., Smith, M.E., Singer, I.A., 1974. Temporal and spatial variation in sulfur dioxide concentrations on suburban Long Island, New York. J. Air Pollut. Control Assoc. 24, 586–590.

Rohde, R.A., Muller, R.A., 2015. Air pollution in China: mapping of concentrations and sources. PLoS one 10, e0135749.

Roth, J., 2022. Pre-test with caution: Event-study estimates after testing for parallel trends. Am. Econ. Rev.: Insights.

Schreifels, J.J., Fu, Y., Wilson, E.J., 2012. Sulfur dioxide control in China: policy evolution during the 10th and 11th Five-year Plans and lessons for the future. Energy Policy 48, 779–789.

Shapiro, J.S., Walker, R., 2018. Why is pollution from US manufacturing declining? The roles of environmental regulation, productivity, and trade. Am. Econ. Rev. 108, 3814–3854.

Shi, X., Xi, T., Zhang, X., Zhang, Y., 2021. "Moving Umbrella": Bureaucratic transfers and the comovement of interregional investments in China. J. Dev. Econ. 153, 102717.

Shimshack, J.P., 2014. The economics of environmental monitoring and enforcement. Annu. Rev. Resour. Econ. 6, 339–360.

Shimshack, J.P., Ward, M.B., 2008. Enforcement and over-compliance. J. Environ. Econ. Manag. 55, 90–105.

Sun, Y., Zwolińska, E., Chmielewski, A.G., 2016. Abatement technologies for high concentrations of NOx and SO2 removal from exhaust gases: A review. Crit. Rev. Environ. Sci. Technol. 46, 119–142.

Vollaard, B., 2017. Temporal displacement of environmental crime: Evidence from marine oil pollution. J. Environ. Econ. Manag. 82, 168–180.

Wu, C., Lu, W., Mei, Y., Yu, B., 2015. Application and running economic analysis of wet flue gas desulfurization technology. Chem. Indus. Eng. Progr. 34, 4368–4374.

Xiang, Y., Zhang, T., Liu, J., Lv, L., Dong, Y., Chen, Z., 2019. Atmosphere boundary layer height and its effect on air pollutants in Beijing during winter heavy pollution. Atmos. Res. 215, 305–316.

Zhang, Y.-L., Cao, F., 2015. Fine particulate matter (PM2. 5) in China at a city level. Sci. Rep. 5, 1–12.
Zhang, B., Chen, X., Guo, H., 2018a. Does central supervision enhance local environmental enforcement? Quasi-experimental evidence from China. J. Public Econ. 164, 70–90.
Zhang, X., Chen, X., Zhang, X., 2018b. The impact of exposure to air pollution on cognitive performance. Proc. Natl. Acad. Sci. 115, 9193–9197.
Zheng, S., Wang, J., Sun, C., Zhang, X., Kahn, M.E., 2019. Air pollution lowers Chinese urbanites' expressed happiness on social media. Nat. Hum. Behav. 3, 237–243.
Zou, E.Y., 2021. Unwatched pollution: The effect of intermittent monitoring on air quality. Am. Econ. Rev. 111, 2101–2126.
Zuo, C.V., 2015. Promoting city leaders: the structure of political incentives in China. China Quart. 224, 955–984.